

Vector model in various dimensions

Mikhail Goykhman* and Michael Smolkin†

The Racah Institute of Physics, The Hebrew University of Jerusalem, Jerusalem 91904, Israel

We study behaviour of the critical $O(N)$ vector model with quartic interaction in $2 \leq d \leq 6$ dimensions to the next-to-leading order in the large- N expansion. We derive and perform consistency checks that provide an evidence for the existence of a non-trivial fixed point and explore the corresponding CFT. In particular, we use conformal techniques to calculate the multi-loop diagrams up to and including 4 loops in general dimension. These results are used to calculate a new CFT data associated with the three-point function of the Hubbard-Stratonovich field. In $6 - \epsilon$ dimensions our results match their counterparts obtained within a proposed alternative description of the model in terms of $N + 1$ massless scalars with cubic interactions. In $d = 3$ we find that the OPE coefficient vanishes up to $\mathcal{O}(1/N^{3/2})$ order.

I. INTRODUCTION

In the past elementary particle theory was based on the assumption that nature must be described by a renormalizable quantum field theory. However, a dramatic progress in the realm of critical phenomena revealed that any non-renormalizable theory will look as if it were renormalizable at sufficiently low energies. From this perspective renormalizable theories correspond to a subset of RG flow trajectories for which all but a few of the couplings vanish. In recent years it has become increasingly apparent that renormalizability is not a fundamental physical requirement, and any realistic quantum field theory may contain non-renormalizable as well as renormalizable interactions. In fact, the experimental success of The Standard Model merely imposes a constraint on the characteristic energy scale of any non-renormalizable interaction. In particular, it remains unclear what is the fundamental principle behind the choice of the trajectory corresponding to the real world from the infinite number of possible theories.

One of the admissible ways to address this problem is to demand that the Hamiltonian of the theory belongs to a trajectory which terminates at a fixed point in UV. Theories with this property are called asymptotically safe. This concept was originally introduced by Weinberg [1, 2] as an approach to select physically consistent quantum field theories (QFT). It provided an alternative to

*Electronic address: michael.goykhman@mail.huji.ac.il

†Electronic address: michael.smolkin@mail.huji.ac.il

the standard requirement of renormalizability. The original argument was motivated by an attempt to avoid hitting the Landau pole along the RG flow by imposing a demand that the flow of a QFT terminates at the UV fixed point. Asymptotically safe theories are not necessarily renormalizable in the usual sense. However, they are interacting QFTs with no unphysical singularities at high energies.

Just as the requirement of renormalizability leaves only few possible interaction terms which one is allowed to include in the Lagrangian, so does the requirement of asymptotic safety impose an infinite number of constraints, limiting the number of physically acceptable theories. Indeed, a UV fixed point in general has only finite number of relevant deformations, therefore any asymptotically safe field theory is entirely specified by a finite number of parameters. Some of such theories are represented by a renormalizable field theory at low energies, while others might be non-renormalizable.

Thus, for instance, a scalar field theory respecting $\phi \rightarrow -\phi$ symmetry rules out the possibility of any renormalizable interaction in five dimensions, yet it exhibits a non-trivial UV fixed point with just two relevant deformations in higher dimensions, and therefore it provides an example of asymptotically safe non-renormalizable quantum field theory [1]. An immediate application of the asymptotic safety is related to the problem of quantum gravity [1–4] which is ongoing (see, *e.g.*, [5] and references therein for recent work).

Several techniques for studying UV properties of QFTs in particular and their RG flows in general have been developed. One of the approaches is to perform a dimensional continuation, and subsequently apply a perturbative expansion around the desired integer-valued physical space-time dimension. This is done with the hope that the result will have sufficiently accurate convergence behaviour to be applied to physically meaningful space-time dimensions, such as $d = 3, 4, 5$. In this spirit the Wilson-Fisher fixed point has originally been derived in $4 - \epsilon$ dimensions, in which case at the fixed point the coupling constant is perturbative in ϵ [6]. In the context of asymptotic safety, gravity has been studied in $2 + \epsilon$ dimensions, see [2–4] for some of the early works.

Recently the $O(N)$ vector model of the scalar fields ϕ^a , $a = 1, \dots, N$, and σ with the relevant cubic interactions $\phi^a \phi^a \sigma$ and σ^3 in $d = 6 - \epsilon$ dimensions has been extensively studied perturbatively in ϵ , see *e.g.*, [7, 8]. This model exhibits an IR fixed point, and it was suggested as an alternative description of the critical scalar $O(N)$ model with quartic interaction $(\phi^a \phi^a)^2$. Several consistency checks for this proposal were given [7, 8]. Some of them, such as matching of the coefficients of the three-point functions $\langle \phi^a \phi^b \sigma \rangle$ and $\langle \sigma \sigma \sigma \rangle$ in both theories, fall within a universal class of results obtained for a generic large- N CFT by the methods of conformal bootstrap [9, 10]. However,

some other checks, such as matching of the anomalous dimensions of certain operators in these theories to high order both in ϵ and $1/N$ expansion, are rather non-trivial [7, 8]. Recent work [11] is also dedicated to calculation of non-perturbative imaginary-valued contributions to the scaling dimensions as a result of fluctuations around instanton background.

Large- N expansion suggests another useful and widely applied tool to study non-perturbative aspects of QFTs. A significant part of the large N lore is due to the original observation made by 't Hooft [12] that the $SU(3)$ QCD becomes more tractable when generalized to the $SU(N)$ gauge theory with matter, and considered in the large- N limit (see also [13] and references therein for some of the earlier arguments regarding the accuracy of such an approximation). In the context of the AdS/CFT correspondence the large- N limit of the $SU(N)$ gauge theories has been subsequently related to the weak Newton/string coupling limit of the dual bulk theory in the AdS space [14–16]. Other recent applications of the large- N formalism include studies of the large- N three-dimensional $SU(N)$ gauge theories with the Chern-Simons interaction, and generalizations of these models to study fundamental vector matter at finite temperature and chemical potential (see, *e.g.*, [17–22] and references therein).¹

Some of the earlier ideas related to applications of the large- N methods are due to the work by Parisi (see [24] and references therein), who in particular developed a systematic proof of renormalizability of the $O(N)$ vector model in $4 < d < 6$ dimensions to each order in the $1/N$ expansion. In particular, one can study the $O(N)$ vector model in a physically interesting dimension $d = 5$. Therefore, this model provides a useful testing ground for the formalism of asymptotic safety [1].

Furthermore, it was shown that the large- N approach can meet the dimensional continuation method (see, *e.g.*, [7] for recent developments in this direction), thanks to the simple observation that the IR Wilson-Fisher fixed point in $d = 4 - \epsilon$ dimensions can be analytically continued to obtain perturbative UV fixed point in $d = 4 + \epsilon$ dimensions, albeit the coupling constant at that fixed point is negative-valued, and therefore the theory is unstable [1]. In fact, the work of [7] was partially motivated by an attempt to design a UV completion of the critical $O(N)$ vector model in $4 < d < 6$ dimensions.²

In this work we continue to study the $O(N)$ vector model with quartic interaction $(\phi^a \phi^a)^2$ in

¹ For recent advances in the large- N QED, see *e.g.*, [23].

² It should be noted that the cubic σ^3 theory considered in [7] is still expected to run into instabilities because of the negative mode associated with fluctuations around the instanton background. See [11] for the recent detailed account of the stability issues in this model.

$2 \leq d \leq 6$ dimensions. We scrutinize renormalization in the $d = 5$ case and provide an additional evidence for the asymptotic safety of the model. Our calculations are done to the next-to-leading order in the $1/N$ expansion, and we successfully recover the known anomalous scaling dimensions associated with the UV CFT [9, 10, 25, 26]. The calculations can be readily extended to general d , and therefore similar conclusions hold for the IR CFT in $2 < d < 4$ as well as for the UV CFT in $4 < d < 6$.

The primary goal of this work is to derive a CFT data associated with the three-point functions $\langle \phi^a \phi^b s \rangle$ and $\langle sss \rangle$ to the next-to-leading order in the $1/N$ expansion. In order to find the $\langle sss \rangle$ three-point function at the $\mathcal{O}(1/N^{3/2})$ order we calculate the 4-loop triangle diagram, and the associated 3-loop trapezoid diagram, as well as the three-loop bellows diagram, in general dimension d . To the best of our knowledge analytic expressions for these diagrams were not presented in the literature before. The results for the $\langle \phi^a \phi^b s \rangle$ agree with [9, 10], whereas the $\mathcal{O}(1/N^{3/2})$ result for $\langle sss \rangle$ is new. This data is important to carve a CFT which describes the critical vector model in general dimension. Setting $d = 6 - \epsilon$ we compare our findings with their counterparts obtained in [7, 8] for the critical cubic model. We find that the OPE coefficients of the $\langle sss \rangle$ three-point functions of these CFTs match at the next-to-leading order in the $1/N$ expansion. We discuss the significance of this non-trivial match in the context of the non-Lagrangian bootstrap approach to the large- N CFTs with $O(N)$ symmetry.

The rest of this paper is organized as follows. In section II we define the model studied in this work and set our notation. Next we assume existence of the fixed point and derive a general relation between the counterterms at the fixed point. In what follows this relation is used as a consistency check for the existence of the fixed point. In section III we focus on the model in 5D. We calculate various counterterms and provide additional evidence in favor of the asymptotic safety of the model. In section IV we review diagrammatic and computational techniques for a CFT in general d , and use them to evaluate various anomalous dimensions and amplitudes of the two-point functions. In section V we calculate the three-point functions associated with a CFT that emerges at the fixed point of the model in $2 \leq d \leq 6$ dimensions. We discuss our results in section VI.

II. SETUP

In this paper we focus on a d -dimensional Euclidean vector model governed by the bare action

$$S = \int d^d x \left(\frac{1}{2} (\partial_\mu \phi)^2 + \frac{1}{2} g_2 \phi^2 + \frac{g_4}{N} (\phi^2)^2 \right), \quad (1)$$

where the field ϕ has N components, but we suppress the vector index for brevity. We keep the dimension d general most of the time, however, some of the specific calculations are carried out in $d = 5$ and $d = 6 - \epsilon$. The behaviour of the model at the fixed point is our main objective, but for now we keep the mass parameter g_2 to preserve generality.

The straightforward and well-known approach (sometimes referred to as the Hubbard-Stratonovich transformation) to study the model such as (1) is to introduce the auxiliary field s which has no impact on the original path integral,

$$S = \int d^d x \left(\frac{1}{2} (\partial_\mu \phi)^2 + \frac{1}{2} g_2 \phi^2 + \frac{g_4}{N} (\phi^2)^2 - \frac{1}{4g_4} \left(s - \frac{2g_4}{\sqrt{N}} \phi^2 \right)^2 \right). \quad (2)$$

After a straightforward simplification this action takes the form

$$S = \int d^d x \left(\frac{1}{2} (\partial_\mu \phi)^2 + \frac{1}{2} g_2 \phi^2 - \frac{1}{4g_4} s^2 + \frac{1}{\sqrt{N}} s \phi^2 \right). \quad (3)$$

As usual, the model (3) has to be renormalized.

To begin with, we introduce the renormalized fields $\tilde{\phi}$, \tilde{s}

$$\phi = \sqrt{Z_\phi} \tilde{\phi}, \quad s = \sqrt{Z_s} \tilde{s}, \quad (4)$$

where the field strength renormalization constants $Z_{\phi,s}$ are expressed in terms of the counterterms $\delta_{\phi,s}$ as

$$Z_\phi = 1 + \delta_\phi, \quad Z_s = 1 + \delta_s. \quad (5)$$

Similarly, the renormalized mass m and coupling \tilde{g}_4 are defined by

$$g_2 Z_\phi = m^2 + \delta_m, \quad (6)$$

$$g_4 Z_\phi^2 = \tilde{g}_4 + \delta_4, \quad (7)$$

where δ_m and δ_4 are mass and quartic coupling counterterms respectively.³

³ It follows from the definition (7) that the interaction term in the original bare action (1) can be expressed as the following sum

$$g_4 (\phi^2)^2 = \tilde{g}_4 (\tilde{\phi}^2)^2 + \delta_4 (\tilde{\phi}^2)^2. \quad (8)$$

It turns out that all counterterms vanish to leading order in the $1/N$ expansion. Therefore to carry out calculations to the next-to-leading order, it is sufficient to linearize the full action with respect to various counterterms. The action (3) in terms of the renormalized parameters is thus given by

$$S = \int d^d x \left(\frac{1}{2} (\partial_\mu \tilde{\phi})^2 + \frac{1}{2} m^2 \tilde{\phi}^2 + \frac{1}{2} \delta_\phi (\partial_\mu \tilde{\phi})^2 + \frac{1}{2} \delta_m \tilde{\phi}^2 - \frac{1}{4\tilde{g}_4} \left(1 + 2\delta_\phi + \delta_s - \frac{\delta_4}{\tilde{g}_4} \right) \tilde{s}^2 + \frac{1}{\sqrt{N}} \left(1 + \frac{1}{2} \delta_s + \delta_\phi \right) \tilde{s} \tilde{\phi}^2 \right). \quad (9)$$

It is convenient to define the following combinations of the counterterms,

$$\hat{\delta}_s = 2\delta_\phi + \delta_s - \frac{\delta_4}{\tilde{g}_4}, \quad (10)$$

$$\frac{\hat{\delta}_4}{\sqrt{\tilde{g}_4}} = \frac{1}{2} \delta_s + \delta_\phi, \quad (11)$$

in terms of which the action can be rewritten as follows

$$S = \int d^d x \left(\frac{1}{2} (\partial_\mu \tilde{\phi})^2 + \frac{1}{2} m^2 \tilde{\phi}^2 - \frac{1}{4\tilde{g}_4} \tilde{s}^2 + \frac{1}{\sqrt{N}} \tilde{s} \tilde{\phi}^2 + \frac{1}{2} \delta_\phi (\partial_\mu \tilde{\phi})^2 + \frac{1}{2} \delta_m \tilde{\phi}^2 - \frac{1}{4\tilde{g}_4} \hat{\delta}_s \tilde{s}^2 + \frac{1}{\sqrt{N}} \frac{\hat{\delta}_4}{\sqrt{\tilde{g}_4}} \tilde{s} \tilde{\phi}^2 \right). \quad (12)$$

Loop corrections along with renormalization conditions fix the counterterms δ_ϕ , δ_m , $\hat{\delta}_s$, and $\hat{\delta}_4$. Inverting (10), (11) one then obtains

$$\delta_s = 2 \left(\frac{\hat{\delta}_4}{\sqrt{\tilde{g}_4}} - \delta_\phi \right), \quad (13)$$

$$\frac{\delta_4}{\tilde{g}_4} = 2 \frac{\hat{\delta}_4}{\sqrt{\tilde{g}_4}} - \hat{\delta}_s. \quad (14)$$

Finally, renormalization of the quartic coupling constant can be read off (5), (7) and (14)

$$g_4 = \tilde{g}_4 \left(1 + 2 \frac{\hat{\delta}_4}{\sqrt{\tilde{g}_4}} - 2\delta_\phi - \hat{\delta}_s \right) = \tilde{g}_4 \left(1 + \delta_s - \hat{\delta}_s \right), \quad (15)$$

where in the last equality (13) was used.

The Callan-Symanzik equation can be used to find various relations between the counterterms of the theory. In particular, using it for the three-point function $\langle \phi \phi s \rangle$, we argue in Appendix A that at the UV (IR) fixed point in $4 < d < 6$ ($2 < d < 4$) dimensions one obtains

$$\mu \frac{\partial}{\partial \mu} \left(\delta_s - \hat{\delta}_s + 2B\mathcal{L}_s \right) = 0 + \mathcal{O}(1/N^2), \quad (16)$$

where μ is an arbitrary renormalization scale. In section III we explicitly confirm this relation in $d = 5$ at the next-to-leading order in the $1/N$ expansion. We interpret it as a consistency check of the assumption that the theory is asymptotically safe.

Of course, the Callan-Symanzik equation is just a statement about consistency of the calculations at various scales of RG flow, and therefore it holds in any field theory. However, it depends on the beta functions of the couplings which are not known in general dimension. For instance, existence of the fixed point in the ϕ^4 vector model was not verified directly in general d . This is just an assumption based on accumulated evidence rather than a derived fact. In particular, eq. (16) is the Callan-Symanzik equation with beta functions suppressed by hand. Yet, it is satisfied by the remaining counterterms which are calculated separately. In this sense (16) plays a role of the consistency check for the existence of a fixed point.

III. UV FIXED POINT IN $d = 5$

A vast amount of literature, starting from the earlier works [1, 24], is dedicated to studying the properties of the UV conformal fixed point of the $O(N)$ vector models with quartic interaction in $4 < d < 6$. While the quartic interaction is non-renormalizable in $d > 4$, one can take advantage of the fact that this model is renormalizable at each order in the $1/N$ expansion [24]. In this section we consider (12) in $d = 5$ dimensions. The main goal is to systematically derive various anomalous dimensions [9, 10, 25, 26] and to verify explicitly that they satisfy certain constraints which are expected to hold at the fixed point. The calculations are carried out to the next-to-leading order in the $1/N$ expansion.

To begin with, we list all necessary Feynman rules for the model (12). A solid line will be used to denote the propagators of various components of the scalar field ϕ , whereas a dashed line is associated with the propagator of the Hubbard-Stratonovich auxiliary field s . Obviously, the matrix of propagators is diagonal, whereas each non-trivial interaction vertex carries two identical vector indices. Hence, for simplicity we suppress the Kronecker delta which explicitly emphasizes these facts. We also omit the momentum conservation delta function at each vertex. Vertices are denoted by a solid blob, whereas propagators are enclosed by black dots (absence of dots indicates an amputated external leg).

$$\begin{array}{ll}
\text{---} \overset{p}{\bullet} \text{---} = \frac{1}{p^2+m^2} & \text{---} \overset{p}{\bullet} \text{---} \bullet = -2\tilde{g}_4 \\
\text{---} \overset{p}{\otimes} \text{---} = -\delta_\phi p^2 - \delta_m & \text{---} \text{---} \otimes = \delta_0 \\
\text{---} \text{---} \bullet \begin{array}{l} / \\ / \\ \backslash \\ \backslash \end{array} = -\frac{2}{\sqrt{N}} & \text{---} \text{---} \otimes \begin{array}{l} / \\ / \\ \backslash \\ \backslash \end{array} = -\frac{2}{\sqrt{N}} \frac{\hat{\delta}_4}{\sqrt{g_4}}
\end{array}$$

Note that we introduced a counterterm δ_0 . It is completely determined by the renormalization condition $\langle \tilde{s} \rangle = 0$. In what follows we assume this condition has been satisfied without elaborating the details.

The full propagator of the Hubbard-Stratonovich field \tilde{s} to leading order in the $1/N$ expansion is thus given by an infinite sum of bubble diagrams

$$\text{---} \text{---} \bullet + \bullet \text{---} \bullet \text{---} \bullet + \bullet \text{---} \bullet \text{---} \bullet \text{---} \bullet \text{---} \bullet + \dots$$

This is a geometric series which can be readily written in a closed form.⁴ We denote it by $G_s(p)$ and represent it diagrammatically by a wavy line

$$\text{---} \overset{p}{\text{wavy}} \text{---} = G_s(p) = -2\tilde{g}_4 \sum_{n=0}^{\infty} (-4\tilde{g}_4 B)^n = \frac{-2\tilde{g}_4}{1+4\tilde{g}_4 B},$$

where each bubble in the infinite series is associated with a UV divergent loop integral

$$B(p) = \int \frac{d^5 q}{(2\pi)^5} \frac{1}{(q^2 + m^2)((p+q)^2 + m^2)}. \quad (17)$$

To regularize the UV divergence we introduce a spherically symmetric sharp cutoff Λ

$$B(p) = \frac{\Lambda}{12\pi^3} - \frac{1}{64\pi^2 p} \left((4m^2 + p^2) \tan^{-1} \left(\frac{p}{2|m|} \right) + 2|m|p \right). \quad (18)$$

The power law divergence can be eliminated by adjusting the counterterm $\hat{\delta}_s$. Unlike logarithmic divergences, the power law divergences depend on the details of regularization scheme. For instance, they are absent in dimensional regularization. Hence, we simply ignore such divergences in what

⁴ One should take into account that each bubble comes with the symmetry factor $1/2$.

is finite. Introducing a sharp cutoff Λ and focusing on the logarithmic divergences only, yields⁵

$$\delta_\phi = -\frac{1}{N} \frac{64}{15\pi^2} \log\left(\frac{\Lambda}{\mu}\right), \quad (22)$$

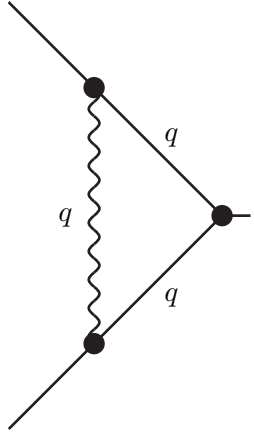
where μ is an arbitrary renormalization scale. The anomalous dimension of the scalar field ϕ at the UV fixed point can be readily evaluated using the Callan-Symanzik equation for the two-point function of $\tilde{\phi}$, see Appendix A

$$\gamma_\phi = \frac{1}{2} \frac{\partial}{\partial \log \mu} \delta_\phi = \frac{1}{N} \frac{32}{15\pi^2}. \quad (23)$$

This result is in full agreement with [9, 10, 25, 26].

B. Renormalization of the interaction vertex

There are two loop diagrams that contribute to renormalization of the interaction vertex at the next to leading order in the $1/N$ expansion. To calculate the corresponding counterterm $\hat{\delta}_4$ it is enough to set all external momenta to zero. The first diagram takes the form

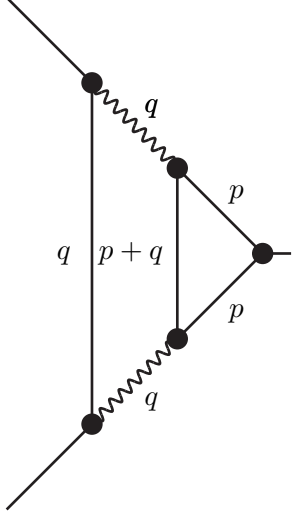


$$= \left(-\frac{2}{\sqrt{N}}\right)^3 \int \frac{d^5 q}{(2\pi)^5} \frac{-1}{2B(q)} \frac{1}{(q^2)^2} = -\frac{1}{N^{3/2}} \frac{128}{3\pi^2} \log \Lambda$$

whereas the second diagram is given by

⁵ If we keep the mass in the action (12), then there is an additional counterterm of the form

$$\delta_m = -\frac{1}{N} \frac{320m^2}{3\pi^2} \log\left(\frac{\Lambda}{\mu}\right). \quad (21)$$



$$= \left(-\frac{2}{\sqrt{N}}\right)^5 N \int \frac{d^5 q}{(2\pi)^5} \left(\frac{-1}{2B(q)}\right)^2 \frac{1}{q^2} \left(-\frac{1}{2}\right) \frac{\partial B(q)}{\partial m^2} = -\frac{1}{N^{3/2}} \frac{512}{3\pi^2} \log \Lambda ,$$

where we used (17) to get the following simple relation

$$-\frac{1}{2} \frac{\partial B(q)}{\partial m^2} = \int \frac{d^5 p}{(2\pi)^5} \frac{1}{(p^2 + m^2)^2 ((p+q)^2 + m^2)}. \quad (24)$$

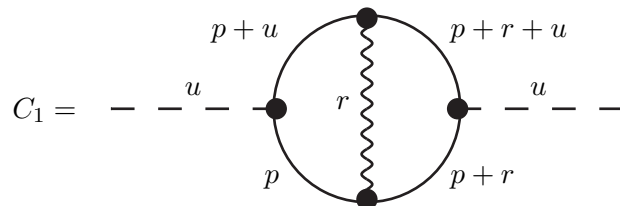
In particular, the loop integral can be calculated by taking derivative of (18) with respect to the mass parameter.

Finally, the tree level counterterm contribution can be read off the Feynman rules we listed in the beginning of this section. Combining everything together and demanding cancellation of the divergences, we obtain

$$\frac{\hat{\delta}_4}{\sqrt{\hat{g}_4}} = -\frac{1}{N} \frac{320}{3\pi^2} \log\left(\frac{\Lambda}{\mu}\right). \quad (25)$$

C. Auxiliary field propagator

Next let us evaluate the counterterm $\hat{\delta}_s$. To this end, we perform renormalization of the Hubbard-Stratonovich propagator. There are five loop diagrams which contribute at the next to leading order in the $1/N$ expansion. We tag these diagrams with C_i , $i = 1, \dots, 5$ and denote their external momentum by u . For simplicity, all the diagrams are amputated, *i.e.*, the two external s propagators are factored out. Thus, for instance



$$C_1 = \text{---} \text{---} \text{---} \text{---}$$

Performing integration over q and keeping the logarithmic divergence only⁶, yields

$$C_3 = -\frac{1}{N} \frac{256}{15\pi^2} B(u) \log \Lambda + \dots \quad (31)$$

The two remaining diagrams are

$$C_4 = 2 \times \text{---} \overset{u}{\text{---}} \text{---} \text{---} \begin{array}{c} p \\ \circlearrowleft \\ \text{---} \text{---} \text{---} \\ p+u \end{array} \text{---} \overset{u}{\text{---}} \text{---} \text{---}$$

and

$$C_5 = \text{---} \overset{u}{\text{---}} \text{---} \text{---} \begin{array}{c} p \\ \otimes \\ \circlearrowleft \\ \text{---} \text{---} \text{---} \\ p+u \end{array} \text{---} \overset{u}{\text{---}} \text{---} \text{---}$$

An extra factor of two in C_4 comes from the interchange of the ordinary vertex with the counterterm. More specifically, the integral expressions for these diagrams read

$$C_4 = 2 \times \frac{1}{2} \left(-\frac{2}{\sqrt{N}} \right) \left(-\frac{2}{\sqrt{N}} \frac{\hat{\delta}_4}{\sqrt{\hat{g}_4}} \right) N \int \frac{d^5 p}{(2\pi)^5} \frac{1}{p^2(p+u)^2} = 4 \frac{\hat{\delta}_4}{\sqrt{\hat{g}_4}} B(u), \quad (32)$$

$$C_5 = \left(-\frac{2}{\sqrt{N}} \right)^2 N \int \frac{d^5 p}{(2\pi)^5} \frac{-p^2 \delta_\phi}{(p^2)^2(p+u)^2} = -4\delta_\phi B(u). \quad (33)$$

Combining the loop diagrams (27), (29), (31), (32), (33) results in the total loop correction to the $\langle \tilde{s}\tilde{s} \rangle$ propagator⁷

$$\mathcal{L}_s = \left(-\frac{1}{2B} \right)^2 \sum_{i=1}^5 C_i = \frac{1}{B} \frac{1}{N} \frac{512}{5\pi^2} \log \frac{\mu}{\mu_0}. \quad (34)$$

It satisfies

$$B \mu \frac{\partial}{\partial \mu} \mathcal{L}_s = -\mu \frac{\partial}{\partial \mu} \left(\frac{\hat{\delta}_4}{\sqrt{\hat{g}_4}} - \delta_\phi \right) \quad (35)$$

Notice that \mathcal{L}_s is finite (the logarithmically divergent terms cancelled out), and therefore

$$\hat{\delta}_s = 0. \quad (36)$$

⁶ Recall that we ignore scheme dependent power law divergences.

⁷ μ_0 is an arbitrary IR scale.

Using the relation (13) we can re-write (35) as

$$\mu \frac{\partial}{\partial \mu} (\delta_s + 2B\mathcal{L}_s) = 0. \quad (37)$$

Our calculations (36), (37) in $d = 5$ agree with the general expression (16). As discussed at the end of section II we interpret it as a consistency check of the assumption that the model is asymptotically safe.

Finally, using the Callan-Symanzik equation for the two-point function of \tilde{s} , see Appendix A, we derive the anomalous dimension of the auxiliary field \tilde{s} to $\mathcal{O}(1/N)$ order,

$$\gamma_s = \frac{1}{2} \mu \frac{\partial}{\partial \mu} (\hat{\delta}_s + 2B\mathcal{L}_s) = \frac{1}{N} \frac{512}{5\pi^2}. \quad (38)$$

This result agrees with the literature [9, 10, 25, 26] and serves as a check of the calculation.

IV. POSITION SPACE CALCULATION IN GENERAL DIMENSION

In the previous section we focused on providing an evidence for the existence of UV fixed point in the 5D vector model. Our next goal is to derive a new CFT data associated with the model at criticality in $2 \leq d \leq 6$. The stage is set in this section, whereas the new results are presented and derived in section V.

We start from calculating the next-to-leading $\mathcal{O}(\frac{1}{N})$ order corrections to the CFT propagators of the fundamental scalar field ϕ and the auxiliary Hubbard-Stratonovich field s , working in position space at the UV fixed point. Space-time dimension d will be assumed to be general $4 < d < 6$ in this section, albeit the results are also applicable to the IR conformal fixed point in $2 < d < 4$ dimensions. To leading order in the large- N expansion the propagators are given by (to avoid clutter we continue to suppress the $O(N)$ vector indices and the explicit factors of the Kronecker delta)

$$\langle \phi(x_1)\phi(x_2) \rangle = C_\phi \frac{1}{|x_{12}|^{2\Delta_\phi}}, \quad (39)$$

$$\langle s(x_1)s(x_2) \rangle = C_s \frac{1}{|x_{12}|^{2\Delta_s}}, \quad (40)$$

where $x_{12} = x_1 - x_2$ and the amplitudes $C_{\phi,s}$ are specified below. To calculate the sub-leading corrections we employ the technique developed in [25–27], following recent developments in [28] (see also [29–32] for an extensive review and discussion of the $1/N$ calculations). The $1/N$ corrections

dress the above propagators. As a result, their form is modified as follows

$$\langle \phi(x_1)\phi(x_2) \rangle = C_\phi(1 + A_\phi) \frac{\mu^{-2\gamma_\phi}}{|x_{12}|^{2(\Delta_\phi + \gamma_\phi)}}, \quad (41)$$

$$\langle s(x_1)s(x_2) \rangle = C_s(1 + A_s) \frac{\mu^{-2\gamma_s}}{|x_{12}|^{2(\Delta_s + \gamma_s)}}, \quad (42)$$

where μ is an arbitrary renormalization scale, $\gamma_{\phi,s}$ represent anomalous dimensions, whereas the symbols $\Delta_{\phi,s}$ stand for the scaling dimensions of the fields ϕ and s at the gaussian fixed point,

$$\Delta_\phi = \frac{d}{2} - 1, \quad \Delta_s = 2, \quad 2\Delta_\phi + \Delta_s = d. \quad (43)$$

While we have already derived the anomalous dimensions $\gamma_{\phi,s}$ in section II for the five dimensional model, in this section we calculate both the anomalous dimensions and the amplitudes $A_{\phi,s}$ in general dimension d . Our findings in this section are in full agreement with the known results in the literature, *e.g.*, [33], and therefore the reader familiar with the subject can proceed to the next section.

A. Preliminary remarks

Performing the Fourier transform

$$\int \frac{d^d k}{(2\pi)^d} e^{ik \cdot x} \frac{1}{(k^2)^{\frac{d}{2} - \Delta}} = \frac{2^{2\Delta - d}}{\pi^{\frac{d}{2}}} \frac{\Gamma(\Delta)}{\Gamma(\frac{d}{2} - \Delta)} \frac{1}{|x|^{2\Delta}}, \quad (44)$$

we find the coefficient C_ϕ in (41)

$$C_\phi = \frac{1}{4\pi^{\frac{d}{2}}} \Gamma\left(\frac{d}{2} - 1\right). \quad (45)$$

Using expression (20) for the s -propagator in momentum space, as well as the result for the bubble loop integral B in general d

$$B(p) = \int \frac{d^d q}{(2\pi)^d} \frac{1}{q^2(p+q)^2} = -\frac{(p^2)^{\frac{d}{2}-2}}{2^d (4\pi)^{\frac{d-3}{2}} \Gamma\left(\frac{d-1}{2}\right) \sin\left(\frac{\pi d}{2}\right)} \quad (46)$$

we obtain ⁸

$$C_s = \frac{2^d \Gamma\left(\frac{d-1}{2}\right) \sin\left(\frac{\pi d}{2}\right)}{\pi^{\frac{3}{2}} \Gamma\left(\frac{d}{2} - 2\right)}. \quad (47)$$

Let us now review the Feynman rules for a CFT in position space [25–27]. At the conformal fixed point, there is no need to keep separate notation (solid or dashed lines) for the propagators of ϕ and s . Instead, we put the power index $2a$ (determined by the scaling dimension a of the corresponding field) on top of the line. The line itself is assumed to be normalized to unity.

⁸ It agrees with [7] after reconciling conventions for normalization of the Hubbard-Stratonovich field.

$$x_1 \overset{2a}{\text{---}} x_2 = \frac{1}{|x_{12}|^{2a}}$$

In particular, the calculation of each diagram starts from counting and writing down explicitly all the factors of $C_{\phi,s}$. The loop diagram in position space simply amounts to adding two powers together.

$$\begin{array}{c} 2a \\ \text{---} \\ \text{---} \\ \text{---} \\ 2b \end{array} = \text{---}^{2(a+b)}$$

We also need the propagator splitting/merging relation [25–27]

$$\int d^d x_3 \frac{1}{(x_3^2)^a ((x_3 - x_{12})^2)^b} = U(a, b, d - a - b) \frac{1}{(x_{12}^2)^{a+b-\frac{d}{2}}}, \quad (48)$$

where

$$U(a, b, c) = \pi^{\frac{d}{2}} \frac{\Gamma(\frac{d}{2} - a) \Gamma(\frac{d}{2} - b) \Gamma(\frac{d}{2} - c)}{\Gamma(a)\Gamma(b)\Gamma(c)}. \quad (49)$$

Expression (48) can be graphically represented as

$$\text{---}^{2a} \bullet \text{---}^{2b} = \text{---}^{2(a+b)-d} \times U(a, b, d - a - b)$$

where the middle point on the l.h.s. is an integrated over vertex. Additionally, we will make use of the following identity for $a_1 + a_2 + a_3 = d$, also known as the uniqueness relation [25–27, 34–37]

$$\int d^d x \frac{1}{|x_1 - x|^{2a_1} |x_2 - x|^{2a_2} |x_3 - x|^{2a_3}} = \frac{U(a_1, a_2, a_3)}{|x_{12}|^{d-2a_3} |x_{13}|^{d-2a_2} |x_{23}|^{d-2a_1}}, \quad (50)$$

where the function U is defined in (49). The uniqueness relation can be represented diagrammatically as [25–27]

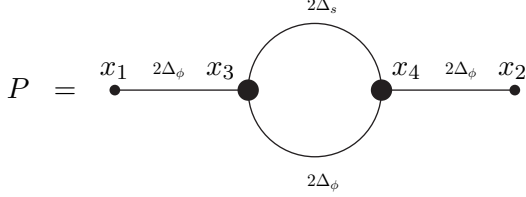
$$\begin{array}{c} \text{---}^{2a_2} \\ \text{---} \\ \text{---}^{2a_1} \end{array} \bullet \text{---}^{2a_3} = \alpha \begin{array}{c} \gamma \\ \text{---} \\ \beta \end{array} \times \left(-\frac{2}{\sqrt{N}}\right) U(a_1, a_2, a_3)$$

where the middle vertex on the l.h.s. is assumed to be integrated over, and we introduced $\alpha = d - 2a_3$, $\beta = d - 2a_2$, $\gamma = d - 2a_1$. Here we also accounted for the Feynman rule associated with the cubic vertex.

$$\begin{array}{c} \text{---} \\ \text{---} \\ \text{---} \end{array} \bullet \text{---} = -\frac{2}{\sqrt{N}}$$

B. ϕ propagator

Let us consider the $1/N$ correction to the ϕ propagator. It is given by the following 1-loop diagram



This diagram reveals a simplest application of the Feynman rules formulated in the previous subsection. It diverges in any d , and therefore we regularize it by adding $\delta/2 \ll 1$ to the scaling dimension of s [25–27]. In other words, we analytically continue the diagram in Δ_s rather than in d . Applying the merging relation (48) twice, yields

$$\begin{aligned}
 P(x_1, x_2) &= \left(-\frac{2}{\sqrt{N}}\right)^2 C_\phi^3 C_s \mu^{-\delta} \int d^d x_{3,4} \frac{1}{|x_{13}|^{2\Delta_\phi} |x_{24}|^{2\Delta_\phi} |x_{34}|^{2\Delta_\phi + 2\Delta_s + \delta}} \\
 &= \frac{4}{N} C_\phi^3 C_s \mu^{-\delta} U\left(\Delta_\phi, \Delta_\phi + \Delta_s + \frac{\delta}{2}, -\frac{\delta}{2}\right) \int d^d x_3 \frac{1}{|x_{13}|^{2\Delta_\phi} |x_{23}|^{d+\delta}} \\
 &= \frac{4}{N} C_\phi^3 C_s \mu^{-\delta} U\left(\Delta_\phi, \Delta_\phi + \Delta_s + \frac{\delta}{2}, -\frac{\delta}{2}\right) U\left(\Delta_\phi, \frac{d+\delta}{2}, \frac{d-\delta}{2} - \Delta_\phi\right) \frac{1}{|x_{12}|^{2\Delta_\phi + \delta}}.
 \end{aligned} \tag{51}$$

Combining with the free propagator (39) and expanding around $\delta = 0$, we obtain

$$\langle \phi(x_1) \phi(x_2) \rangle = \frac{C_\phi}{|x_{12}|^{2\Delta_\phi}} \left(1 + \left(\frac{2\gamma_\phi}{\delta} + A_\phi + \mathcal{O}(\delta) \right) \frac{1}{(|x_{12}| \mu)^\delta} \right). \tag{52}$$

Here

$$\gamma_\phi = \frac{1}{N} \frac{2^d \sin\left(\frac{\pi d}{2}\right) \Gamma\left(\frac{d-1}{2}\right)}{\pi^{3/2} (d-2) d \Gamma\left(\frac{d}{2} - 2\right)}, \tag{53}$$

$$A_\phi = \gamma_\phi \left(\frac{d}{2-d} - \frac{2}{d} \right). \tag{54}$$

Divergence in the correlation function can be readily removed by the wave function renormalization,

$$\phi = \sqrt{Z_\phi} \tilde{\phi}, \quad Z_\phi = 1 + \frac{2\gamma_\phi}{\delta}. \tag{55}$$

As a result, the correlation function for the physical field $\tilde{\phi}$ to the next-to-leading order in the $1/N$ expansion takes the form (41) with γ_ϕ, A_ϕ given by (53), (54).

Note that γ_ϕ in $d = 5$ agrees with (23), whereas in general d our results match [9, 10, 25, 26, 33]. In particular, the anomalous dimension (53) and the amplitude shift (54) in $d = 6 - \epsilon$ dimensions

are given by

$$\gamma_\phi = \frac{\epsilon}{N} + \mathcal{O}(\epsilon^2), \quad (56)$$

$$A_\phi = -\frac{11\epsilon}{6N} + \mathcal{O}(\epsilon^2). \quad (57)$$

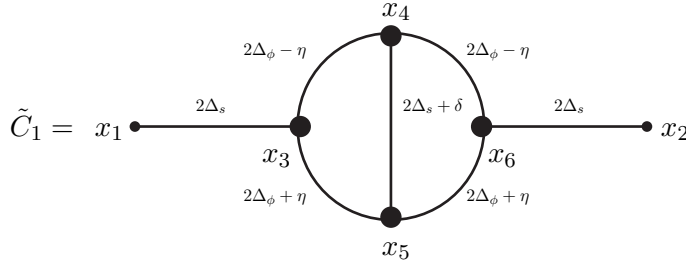
C. Hubbard-Stratonovich propagator

Next we derive the $1/N$ correction to the propagator of the auxiliary field s . As in section III, we have three diagrams $C_{1,2,3}$. Furthermore, since the model is regulated by analytic continuation in the scaling dimension of the fields, there is no need to introduce explicitly the counterterm diagrams $C_{4,5}$ of section III. They are associated with the wave function renormalization and we merely implement it at the end of calculation.

For each diagram we begin by counting and writing down the prefactor associated with the amplitudes $C_{\phi,s}$. To this end, denote

$$C_1(x_1, x_2) = C_s^3 C_\phi^4 \tilde{C}_1(x_1, x_2) \mu^{-\delta}, \quad (58)$$

where $\tilde{C}_1(x_1, x_2)$ is given by



We introduced an extra power η to the internal lines representing ϕ propagator, see *e.g.*, [25, 26, 38, 39]. Ultimately we are interested in the limit $\eta, \delta \rightarrow 0$. However, this limit can be reliably taken as long as $\eta = \mathcal{O}(\delta)$. Indeed, the resulting diagram is both symmetric w.r.t. $\eta \rightarrow -\eta$ and finite as $\eta \rightarrow 0$, therefore its series expansion around $\eta = 0$ takes the form [28]

$$\tilde{C}_1 = f_0 + f_2 \eta^2 + f_4 \eta^4 + \dots \quad (59)$$

Further expanding it around $\delta = 0$ and keeping in mind that the coefficients f_a have at most simple poles at $\delta = 0$, we conclude that $\tilde{C}_1 = f_0$ in the limit $\delta \rightarrow 0$, as long as $\eta = \mathcal{O}(\delta)$. It is convenient to choose $\eta = \delta/2$. As a result, we obtain

$$\begin{aligned} \tilde{C}_1 &= \frac{1}{2} \left(-\frac{2}{\sqrt{N}} \right)^4 N \int d^d x_{3,6} \frac{1}{(|x_{13}| |x_{26}|)^{2\Delta_s}} \int d^d x_5 \frac{1}{|x_{35}|^{2\Delta_\phi + \frac{\delta}{2}} |x_{56}|^{2\Delta_\phi + \frac{\delta}{2}}} \\ &\times \int d^d x_4 \frac{1}{|x_{34}|^{2\Delta_\phi - \frac{\delta}{2}} |x_{45}|^{2\Delta_s + \delta} |x_{46}|^{2\Delta_\phi - \frac{\delta}{2}}}. \end{aligned} \quad (60)$$

Presence of $\eta = \delta/2$ makes it possible to use the uniqueness equation (50) to integrate over x_4 . Applying subsequently the propagator merging relation (48) to the integral over x_5 , yields

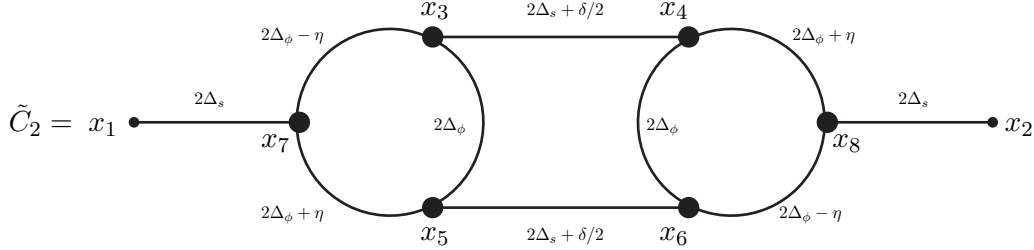
$$\begin{aligned} \tilde{C}_1 &= \frac{8}{N} U \left(\Delta_\phi - \frac{\delta}{4}, \Delta_\phi - \frac{\delta}{4}, \Delta_s + \frac{\delta}{2} \right) U \left(\frac{d+\delta}{2}, \frac{d+\delta}{2}, -\delta \right) \\ &\times \int d^d x_{3,6} \frac{1}{(|x_{13}| |x_{26}|)^{2\Delta_s}} \frac{1}{|x_{36}|^{2d-2\Delta_s+\delta}}. \end{aligned} \quad (61)$$

We postpone carrying out the remaining integrals over the two edge points $x_{3,6}$. Similar integrals appear in the calculation of $C_{2,3}$, and therefore it makes sense to evaluate them after we have assembled all the terms $C_{1,2,3}$ together.

The next diagram contributing to the s propagator at the $\mathcal{O}(1/N)$ order is denoted by

$$C_2(x_1, x_2) = C_s^4 C_\phi^6 \tilde{C}_2(x_1, x_2) \mu^{-\delta}, \quad (62)$$

where



Notice that we regularized this diagram by supplementing the internal s propagators with an additional power of $\delta/2$ rather than δ . This is done in order to ensure the same total compensating power of μ on the r.h.s. of (62) as in C_1 , namely $\mu^{-\delta}$, and therefore such prescription guarantees consistency of regularization of the diagrams [28]. We have also modified some of the ϕ lines, relying on the technique we used in evaluating the diagram \tilde{C}_1 . Setting $\eta = \frac{\delta}{2}$ [38, 39], see also [28], allows us to carry out the integrals over $x_{3,6}$ using the uniqueness relation (50),

$$\begin{aligned} \tilde{C}_2 &= \frac{1}{2} \left(-\frac{2}{\sqrt{N}} \right)^6 N^2 \int d^d x_{7,8} \frac{1}{(|x_{17}| |x_{28}|)^{2\Delta_s}} \int d^d x_{4,5} \frac{1}{|x_{48}|^{2\Delta_\phi + \frac{\delta}{2}} |x_{57}|^{2\Delta_\phi + \frac{\delta}{2}}} \\ &\times \int d^d x_3 \frac{1}{|x_{37}|^{2\Delta_\phi - \frac{\delta}{2}} |x_{34}|^{2\Delta_s + \frac{\delta}{2}} |x_{35}|^{2\Delta_\phi}} \int d^d x_6 \frac{1}{|x_{68}|^{2\Delta_\phi - \frac{\delta}{2}} |x_{56}|^{2\Delta_s + \frac{\delta}{2}} |x_{46}|^{2\Delta_\phi}}. \end{aligned} \quad (63)$$

Integrating over $x_{3,6}$, gives

$$\tilde{C}_2 = \frac{32}{N} U \left(\Delta_\phi - \frac{\delta}{4}, \Delta_s + \frac{\delta}{4}, \Delta_\phi \right)^2 \int d^d x_{7,8} \frac{1}{(|x_{17}| |x_{28}|)^{2\Delta_s}} \tilde{c}_2(x_7, x_8; 0), \quad (64)$$

where

$$\tilde{c}_2(x_7, x_8; \eta') = \int d^d x_{4,5} \frac{1}{|x_{48}|^{2d-3\Delta_s-\eta'} |x_{57}|^{2d-3\Delta_s+\eta'} |x_{45}|^{2\Delta_s+\delta} |x_{47}|^{\Delta_s-\eta'} |x_{58}|^{\Delta_s+\eta'}}. \quad (65)$$

Here we have introduced an additional exponent η' [25, 26, 28] which has little impact on the final value of the diagram. Indeed, by performing the following change of integration variables

$$x_4 \rightarrow x_7 + x_8 - x_5, \quad x_5 \rightarrow x_7 + x_8 - x_4, \quad (66)$$

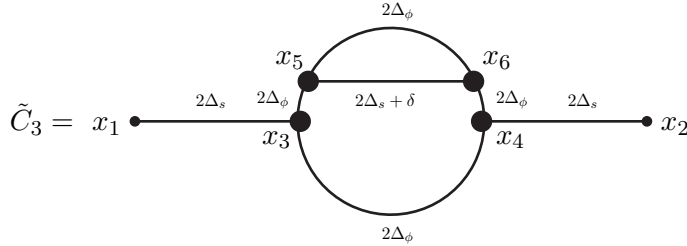
one can see that $\tilde{c}_2(x_7, x_8; \eta') = \tilde{c}_2(x_7, x_8; -\eta')$. Therefore, similarly to the calculation of \tilde{C}_1 , any choice of $\eta' = \mathcal{O}(\delta)$ does not change the value of the diagram in the limit $\delta \rightarrow 0$. Specifically choosing $\eta' = \frac{\delta}{2}$ makes it possible to apply the uniqueness relation (50) to the integral over x_4 [28] followed by the propagator merging relation (48) to the integral over x_5

$$\begin{aligned} \tilde{C}_2 &= \frac{32}{N} U \left(\Delta_\phi - \frac{\delta}{4}, \Delta_s + \frac{\delta}{4}, \Delta_\phi \right)^2 U \left(d - \frac{3\Delta_s}{2} - \frac{\delta}{4}, \Delta_s + \frac{\delta}{2}, \frac{\Delta_s}{2} - \frac{\delta}{4} \right) \\ &\times U \left(\frac{d+\delta}{2}, \frac{d+\delta}{2}, -\delta \right) \int d^d x_{7,8} \frac{1}{(|x_{17}||x_{28}|)^{2\Delta_s}} \frac{1}{|x_{78}|^{2d-2\Delta_s+\delta}}. \end{aligned} \quad (67)$$

Finally, the last diagram is given by

$$C_3(x_1, x_2) = C_s^3 C_\phi^4 \tilde{C}_3(x_1, x_2) \mu^{-\delta}, \quad (68)$$

where



This diagram contains a sub-diagram which was evaluated already, namely, the one-loop correction to the ϕ propagator. Hence, it can be readily simplified

$$\begin{aligned} \tilde{C}_3 &= \frac{16}{N} U \left(\Delta_\phi, \Delta_\phi + \Delta_s + \frac{\delta}{2}, -\frac{\delta}{2} \right) U \left(\Delta_\phi, \frac{d+\delta}{2}, \frac{d-\delta}{2} - \Delta_\phi \right) \\ &\times \int d^d x_{3,4} \frac{1}{(|x_{13}||x_{24}|)^{2\Delta_s}} \frac{1}{|x_{34}|^{2d-2\Delta_s+\delta}}. \end{aligned} \quad (69)$$

Next we combine $C_{1,2,3}$. To begin with, we note that (61), (67), (69) exhibit a similar structure,

$$\tilde{C}_i = \hat{C}_i \int d^d x_{3,4} \frac{1}{(|x_{13}||x_{24}|)^{2\Delta_s}} \frac{1}{|x_{34}|^{2d-2\Delta_s+\delta}}. \quad (70)$$

Using (48) twice to perform the remaining integrals over $x_{3,4}$, yields

$$\tilde{C}_i = U \left(\Delta_s, d - \Delta_s + \frac{\delta}{2}, -\frac{\delta}{2} \right) U \left(\Delta_s, \frac{d+\delta}{2}, \frac{d-\delta}{2} - \Delta_s \right) \hat{C}_i \frac{1}{|x_{12}|^{2\Delta_s+\delta}}. \quad (71)$$

Summing up all three diagrams and expanding around $\delta = 0$ we obtain

$$\langle s(x_1)s(x_2) \rangle = \frac{C_s}{|x_{12}|^{2\Delta_s}} \left(1 + \left(\frac{2\gamma_s}{\delta} + A_s + \mathcal{O}(\delta) \right) \frac{1}{(|x_{12}\mu|)^\delta} \right), \quad (72)$$

with

$$\gamma_s = \frac{1}{N} \frac{4 \sin\left(\frac{\pi d}{2}\right) \Gamma(d)}{\pi \Gamma\left(\frac{d}{2} + 1\right) \Gamma\left(\frac{d}{2} - 1\right)}, \quad (73)$$

$$A_s = 2\gamma_\phi \left(\frac{d(d-3)+4}{4-d} \left(H_{d-3} + \pi \cot\left(\frac{\pi d}{2}\right) \right) + \frac{8}{(d-4)^2} + \frac{2}{d-2} + \frac{2}{d} - 2d - 1 \right), \quad (74)$$

where H_n is the n th harmonic number.

As before, divergence in the correlation function is removed by the wave function renormalization,

$$s = \sqrt{Z_s} \tilde{s}, \quad Z_s = 1 + \frac{2\gamma_s}{\delta}. \quad (75)$$

In particular, the correlation function for the physical field \tilde{s} to the next-to-leading order in the $1/N$ expansion takes the form (42) with γ_s, A_s given by (73), (74).

Notice that the wave function renormalization constants (55), (75) generate the following renormalization of the bare term in the action (3)

$$\frac{1}{\sqrt{N}} \phi^2 s = \frac{1}{\sqrt{N}} \tilde{\phi}^2 \tilde{s} + \frac{2\gamma_\phi + \gamma_s}{\delta} \frac{1}{\sqrt{N}} \tilde{\phi}^2 \tilde{s}, \quad (76)$$

where we keep $\mathcal{O}(1/N)$ corrections only. Thus the counterterm is given by

$$S_{\text{int}}^{\text{c.t.}} = \frac{2\gamma_\phi + \gamma_s}{\delta} \frac{1}{\sqrt{N}} \tilde{\phi}^2 \tilde{s}. \quad (77)$$

To avoid clutter we suppress tilde above the renormalized fields $\tilde{\phi}, \tilde{s}$ in what follows. Of course, physical correlations are associated with the renormalized fields.

Before closing this section we note that γ_s in $d = 5$ agrees with (38), whereas in general d our results match [9, 10, 25, 26, 33]. In particular, the anomalous dimension (73) and the amplitude shift (74) in $d = 6 - \epsilon$ dimensions are given by

$$\gamma_s = \frac{40\epsilon}{N} + \mathcal{O}(\epsilon^2), \quad (78)$$

$$A_s = \frac{44}{N} + \mathcal{O}(\epsilon). \quad (79)$$

V. CONFORMAL THREE-POINT FUNCTIONS

In this section we calculate the next-to-leading order correction to the OPE coefficients of the conformal three-point functions $\langle \phi\phi s \rangle$ and $\langle sss \rangle$ associated with the fundamental scalar field ϕ

and the auxiliary Hubbard-Stratonovich field s . In a general d -dimensional $O(N)$ symmetric CFT, the results for $\langle\phi\phi s\rangle$ to the next-to-leading order and leading order $\langle sss\rangle$ correlator are known based on the conformal bootstrap approach [9, 10] (see also [40, 41] for discussion in the context of $O(N)$ sigma model). In contrast, we recover these results in the critical ϕ^4 model from the new perspective which has not previously been given in the literature, and extend the calculations to derive a new OPE coefficient of the three-point function $\langle sss\rangle$.

Furthermore, to facilitate and make progress in the calculations we evaluate the 4-loop conformal triangle diagram, and the associated 3-loop trapezoid graph, as well as the 3-loop bellows diagram in general dimension d . To the best of our knowledge, these diagrams were not evaluated in the literature before, and the corresponding analytic expressions were not displayed elsewhere. These diagrams naturally appear in numerous conformal calculations, and therefore might be useful in the future.

A. $\langle\phi\phi s\rangle$

The leading order result for the $\langle\phi\phi s\rangle$ correlator follows directly from the tree-level diagram,

$$\langle\phi(x_1)\phi(x_2)s(x_3)\rangle\Big|_{\text{leading}} = -\frac{2}{\sqrt{N}}C_\phi^2C_s \int d^d x \frac{1}{|x_1-x|^{2\Delta_\phi}|x_2-x|^{2\Delta_\phi}|x_3-x|^{2\Delta_s}}. \quad (80)$$

Using the uniqueness relation (50) we obtain the conformal three-point function

$$\langle\phi(x_1)\phi(x_2)s(x_3)\rangle\Big|_{\text{leading}} = \frac{C_{\phi\phi s}}{|x_{12}|^{2\Delta_\phi-\Delta_s}|x_{13}|^{\Delta_s}|x_{23}|^{\Delta_s}}, \quad (81)$$

where the leading order coefficient is given by

$$C_{\phi\phi s} = -\frac{2}{\sqrt{N}}C_\phi^2C_s U(\Delta_\phi, \Delta_\phi, \Delta_s). \quad (82)$$

It is convenient to express the three-point functions in terms of normalized fields

$$\phi \rightarrow \phi \sqrt{C_\phi(1+A_\phi)}, \quad s \rightarrow s \sqrt{C_s(1+A_s)}, \quad (83)$$

i.e., fields whose two-point functions are normalized to unity. The OPE coefficient, $\tilde{C}_{\phi\phi s}$, associated with the renormalized fields is given by⁹

$$\tilde{C}_{\phi\phi s} = \frac{C_{\phi\phi s}}{C_\phi C_s^{\frac{1}{2}}}, \quad (84)$$

⁹ We ignore $A_{\phi,s}$ in (83) to leading order in the $1/N$ expansion.

where the grey blob in the center represents a dressed three-point vertex.¹¹ By conformal invariance this diagram takes the form

$$\langle \phi(x_1)\phi(x_2)s(x_3) \rangle = \tilde{C}_{\phi\phi s} \frac{(1 + W_{\phi\phi s})\mu^{-2\gamma_\phi - \gamma_s}}{|x_{12}|^{2(\Delta_\phi + \gamma_\phi) - (\Delta_s + \gamma_s)} |x_{13}|^{\Delta_s + \gamma_s} |x_{23}|^{\Delta_s + \gamma_s}}, \quad (87)$$

where the fields ϕ and s are normalized such that their two-point function has unit amplitude. Our goal is to calculate $W_{\phi\phi s}$ to order $\mathcal{O}(\frac{1}{N})$. It represents a subleading correction to the OPE coefficient $\tilde{C}_{\phi\phi s}$.

The dressed 1PI vertex, $\Gamma(x, y, z)$, in the above diagram was evaluated in [33] to $\mathcal{O}(1/N)$ order, see eq. (4.18) there,

$$\int \int \int \Gamma(x_1, x_2, x_3)\phi(x_1)\phi(x_2)s(x_3) = \frac{\hat{Z}}{\sqrt{N}} \int \int \int \frac{\mu^{-2\gamma_\phi - \gamma_s} \phi(x_1)\phi(x_2)s(x_3)}{|x_3 - x_1|^{2\alpha} |x_3 - x_2|^{2\alpha} |x_1 - x_2|^{2\beta}}, \quad (88)$$

where in notations of [33]

$$\alpha = \Delta_\phi - \frac{\gamma_s}{2}, \quad \beta = \Delta_s - \gamma_\phi + \frac{\gamma_s}{2}, \quad (89)$$

and \hat{Z} is a constant given by eq. (A.4) in [33]¹²

$$\begin{aligned} \hat{Z} &= -\frac{\chi}{2} \frac{A(1)^2 A(\tilde{\mu} - 2) \Gamma(\tilde{\mu})}{\pi^{2\tilde{\mu}}} (1 + \delta V'), \quad \chi = -(2\gamma_\phi + \gamma_s), \\ A(\Delta) &= \frac{\Gamma(\frac{d}{2} - \Delta)}{\Gamma(\Delta)}, \quad \tilde{\mu} = \frac{d}{2}, \\ \delta V' &= \frac{\eta_1 (\tilde{\mu} - 3) (6\tilde{\mu}^2 - 9\tilde{\mu} + 2)}{N (\tilde{\mu} - 2)^2}, \quad \eta_1 \equiv \frac{4(2 - \tilde{\mu})\Gamma(2\tilde{\mu} - 2)}{\Gamma(\tilde{\mu} - 1)^2 \Gamma(2 - \tilde{\mu}) \Gamma(\tilde{\mu} + 1)}. \end{aligned} \quad (90)$$

To get $W_{\phi\phi s}$ one should simply attach the dressed propagators to $\Gamma(x, y, z)$ and apply the uniqueness formula (50) three times, because all 3 vertices $x_{1,2,3}$ happen to be unique. Normalizing the external legs, yields

$$\tilde{C}_{\phi\phi s} (1 + W_{\phi\phi s}) = -\frac{2}{\sqrt{N}} \frac{C_\phi^2 (1 + A_\phi)^2 C_s (1 + A_s)}{\sqrt{C_\phi^2 (1 + A_\phi)^2 C_s (1 + A_s)}} \hat{Z} \hat{U}, \quad (91)$$

where we defined

$$\begin{aligned} \hat{U} &= U\left(\Delta_\phi - \frac{\gamma_s}{2}, \Delta_\phi - \frac{\gamma_s}{2}, \Delta_s + \gamma_s\right) U\left(\Delta_\phi - \frac{\gamma_s}{2}, \Delta_\phi + \gamma_\phi, \Delta_s - \gamma_\phi + \frac{\gamma_s}{2}\right) \\ &\times U\left(\Delta_\phi + \gamma_\phi, \frac{\Delta_s + \gamma_s}{2}, \frac{d}{2} - \gamma_\phi - \frac{\gamma_s}{2}\right). \end{aligned} \quad (92)$$

¹¹ By definition, the dressed vertex has no propagators attached to the external legs (amputated diagram).

¹² Our notations differ from those of [33]. The precise relation is $\mu \rightarrow \tilde{\mu}$, $\gamma_\psi \rightarrow \gamma_s$, $H(\Delta) \rightarrow A(\Delta)$.

Expansion of \hat{U} in $1/N$ has the following form

$$\hat{U} = N u_1 + u_2 + \mathcal{O}\left(\frac{1}{N}\right). \quad (93)$$

Notice that it starts with the divergent in $N \rightarrow \infty$ piece $N u_1$, originating from the singular in that limit factor $U\left(\frac{d}{2} - \gamma_\phi - \frac{\gamma_s}{2}, \dots\right)$ in (92). It is convenient to denote the ratio of the sub-leading to leading coefficients in (93) by

$$\hat{u} = \frac{u_2}{N u_1} = \frac{\gamma_s((26 - 3d)d - 44) + 2\gamma_\phi((d - 6)d + 4)}{2(d - 4)(d - 2)}. \quad (94)$$

Here the anomalous dimensions γ_ϕ , γ_s are given by (53), (73). Combining \hat{u} with the other next-to-leading order terms in (91), we obtain

$$W_{\phi\phi s} = A_\phi + \frac{A_s}{2} + \delta V, \quad (95)$$

where

$$\delta V = \hat{u} + \delta V' = \frac{1}{N} \frac{2^{d-3}(d(d(5d - 42) + 116) - 96) \sin\left(\frac{\pi d}{2}\right) \Gamma\left(\frac{d-1}{2}\right)}{\pi^{3/2}(d-4)(d-2)\Gamma\left(\frac{d}{2} + 1\right)}, \quad (96)$$

which we can re-write as

$$\delta V = \gamma_\phi \left(\frac{8}{(d-4)^2} + \frac{2}{d-2} + \frac{6}{d-4} + 5 \right), \quad (97)$$

where γ_ϕ is given by (53). Substituting (54), (74) and (97) into (95) gives $W_{\phi\phi s}$ in general dimension. It matches [9, 10] where the generic $O(N)$ symmetric CFT was studied, *e.g.*, see eq. (21) in [9].¹³ In particular, the above $W_{\phi\phi s}$ agrees with its counterpart in a CFT emerging at the IR fixed point of the $O(N)$ vector model with cubic interactions in $d = 6 - \epsilon$ dimensions [7]. In this case one gets

$$\delta V = \frac{1}{N} \frac{21\epsilon}{2} + \mathcal{O}(\epsilon^2), \quad W_{\phi\phi s} = \frac{22}{N} + \mathcal{O}(\epsilon). \quad (99)$$

While this way of calculating $W_{\phi\phi s}$ is straightforward, it does not separate the effect of the anomalous dimensions intrinsic to the propagators from the contribution of the dressed vertex. Such a separation proves to be useful when we evaluate $\langle sss \rangle$ correlation function. In other words, the impact of anomalous dimensions inherent to the propagators is singled out in our method

¹³ Note that the leading terms in the large N expansion on the l.h.s. and r.h.s. of (91) agree, as one can explicitly verify by direct calculation,

$$-\frac{2}{\sqrt{N}} C_\phi C_s^{\frac{1}{2}} \left(-\frac{\chi}{2} \frac{A(1)^2 A(\tilde{\mu} - 2) \Gamma(\tilde{\mu})}{\pi^{2\tilde{\mu}}} \right) N u_1 = -\frac{2}{\sqrt{N}} C_\phi C_s^{\frac{1}{2}} U(\Delta_\phi, \Delta_\phi, \Delta_s) = \tilde{C}_{\phi\phi s}. \quad (98)$$

of calculating the $\langle sss \rangle$ correlation function. Hence, for future purpose we define two additional Feynman rules.

To begin with, we exclude $A_{\phi,s}$ from the residue of the dressed propagators. These constants represent $1/N$ corrections to the amplitudes of the two-point functions and can be accounted at the very end. The dressed propagators without $A_{\phi,s}$ will be denoted by a solid black blob¹⁴

$$\text{---} \bullet \text{---} = C \frac{\mu^{-2\gamma}}{|x|^{2(\Delta+\gamma)}}$$

As before (C, Δ, γ) stand for $(C_{\phi,s}, \Delta_{\phi,s}, \gamma_{\phi,s})$, depending on the considered propagator.

Next we define a dressed vertex with the bare propagators attached to it, *i.e.*, propagators without anomalous dimensions and $A_{\phi,s}$. Diagrammatically it is given by

$$\begin{aligned} & \text{Diagram 1} = C_{\phi\phi s}(1 + \delta V) \text{Diagram 2} - \text{Diagram 3} + \text{Diagram 4} \\ & \text{Diagram 1: A circle with an incoming line of degree } 2\Delta_s \text{ and two outgoing lines of degree } 2\Delta_\phi. \\ & \text{Diagram 2: A triangle with an incoming line of degree } \Delta_s + \gamma_s \text{ and two outgoing lines of degree } \Delta_s + \gamma_s. \\ & \text{Diagram 3: A vertex with an incoming line of degree } 2(\Delta_s + \gamma_s) \text{ and two outgoing lines of degree } 2(\Delta_\phi + \gamma_\phi). \\ & \text{Diagram 4: A vertex with an incoming line of degree } 2\Delta_s \text{ and two outgoing lines of degree } 2\Delta_\phi. \end{aligned} \quad (100)$$

where the external legs are not normalized, and therefore $C_{\phi\phi s}$ rather than $\tilde{C}_{\phi\phi s}$ appears on the r.h.s. The term $\delta V \sim \mathcal{O}(1/N)$ equals $W_{\phi\phi s}$ up to corrections $A_{\phi,s}$ that we stripped off. In fact, δV is closely related to the sum of two loop diagrams, which have been studied in momentum space in section IIIB. Notice that δV is rendered finite, because besides those two loop diagrams there is a contribution from the vertex counterterm (77). The last diagram on the r.h.s. simply subtracts the leading $1/N$ contribution from the second diagram

$$\begin{aligned} & \text{Diagram 3} - \text{Diagram 4} = -\frac{2}{\sqrt{N}} C_\phi^2 C_s \int d^d x_4 \frac{1}{(|x_{14}| |x_{24}|)^{2\Delta_\phi} |x_{34}|^{2\Delta_s}} \left(\frac{2}{\delta \mu^\delta} \left(\frac{\gamma_\phi}{|x_{14}|^\delta} + \frac{\gamma_\phi}{|x_{24}|^\delta} + \frac{\gamma_s}{|x_{34}|^\delta} \right) - 2 \frac{2\gamma_\phi + \gamma_s}{\delta} \right) \end{aligned}$$

where the last term within the parenthesis stands for the counterterm associated with the wave function renormalization (55) and (75), and we used regularized expressions for the dressed propagators obtained previously by the direct calculation of the Feynman graphs. Note that the newly

¹⁴ Note that it is crucial to account for $A_{\phi,s}$, see *e.g.*, (95).

defined vertex with the bare propagators attached to it has logarithmic terms proportional to the anomalous dimensions. Such terms emerge because of renormalization of the vertex, and are intrinsic to the vertex itself rather than to the propagators.

We choose to keep track separately of the contributions associated with the dressed vertex correction δV and anomalous dimensions $\gamma_{\phi,s}$ of the propagators. Hence, the above diagrams will be used extensively in what follows. This approach turns out to be useful when we evaluate the $\langle sss \rangle$ correlation function.

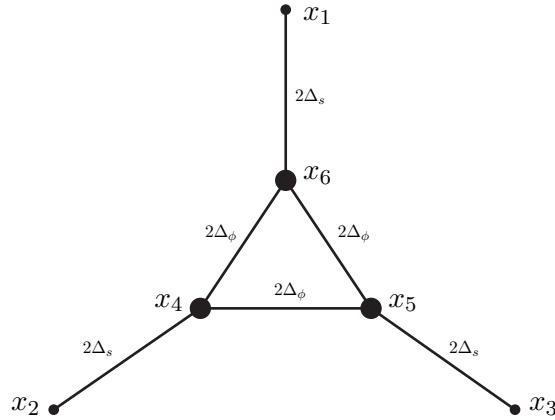
B. $\langle sss \rangle$

In this subsection we calculate the three-point function $\langle sss \rangle$ to $\mathcal{O}\left(\frac{1}{N^{3/2}}\right)$ order. For the normalized field (83) it has the form

$$\langle s(x_1)s(x_2)s(x_3) \rangle = \tilde{C}_{s^3} \frac{(1 + W_{s^3})\mu^{-3\gamma_s}}{|x_{12}|^{\Delta_s+\gamma_s}|x_{13}|^{\Delta_s+\gamma_s}|x_{23}|^{\Delta_s+\gamma_s}}. \quad (101)$$

We are going to calculate the leading coefficient \tilde{C}_{s^3} and the $1/N$ correction W_{s^3} .

The leading behaviour is completely determined by the one-loop triangle diagram



Normalizing the external legs yields

$$\begin{aligned} \langle s(x_1)s(x_2)s(x_3) \rangle \Big|_{\text{leading}} &= N \left(-\frac{2}{\sqrt{N}} \right)^3 \frac{C_\phi^3 C_s^3}{\sqrt{C_s^3}} \int d^d x_{4,5} \frac{1}{|x_{35}|^{2\Delta_s} |x_{45}|^{2\Delta_\phi} |x_{24}|^{2\Delta_s}} \\ &\times \int d^d x_6 \frac{1}{|x_{16}|^{2\Delta_s} |x_{46}|^{2\Delta_\phi} |x_{56}|^{2\Delta_\phi}}. \end{aligned} \quad (102)$$

Applying uniqueness formula (50) to the integrals over $x_{4,5,6}$, we arrive at the leading $\langle sss \rangle$ triangle expression

$$\langle s(x_1)s(x_2)s(x_3) \rangle \Big|_{\text{leading}} = \frac{\tilde{C}_{s^3}}{|x_{12}|^{\Delta_s} |x_{23}|^{\Delta_s} |x_{13}|^{\Delta_s}}, \quad (103)$$

where

$$\tilde{C}_{s^3} = -\frac{8}{\sqrt{N}} C_\phi^3 C_s^{\frac{3}{2}} U(\Delta_\phi, \Delta_\phi, \Delta_s)^2 U\left(\frac{\Delta_s}{2}, \Delta_s, d - \frac{3\Delta_s}{2}\right). \quad (104)$$

One can readily show that for general d

$$C_\phi^2 C_s U(\Delta_\phi, \Delta_\phi, \Delta_s) U\left(\frac{\Delta_s}{2}, \Delta_s, d - \frac{3\Delta_s}{2}\right) = \frac{d-3}{2}, \quad (105)$$

and therefore using (85) we obtain

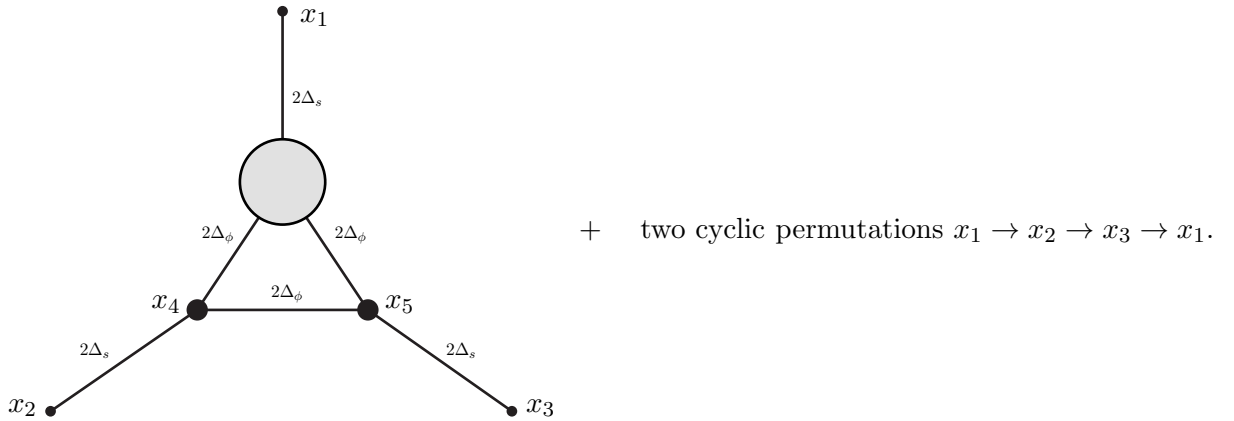
$$\tilde{C}_{s^3} = 2(d-3) \tilde{C}_{\phi\phi s}, \quad (106)$$

in agreement with [9, 10].

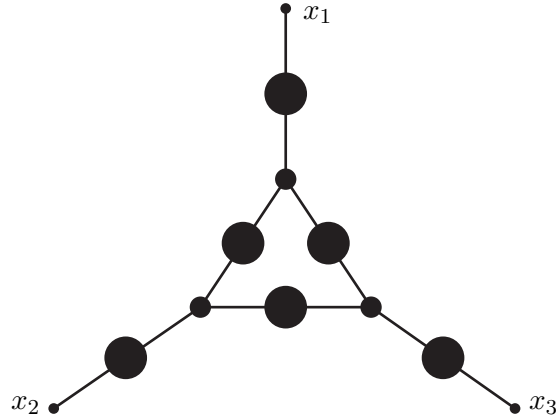
Next we evaluate the sub-leading term W_{s^3} in (101). It is determined by the $\mathcal{O}(1/N^{3/2})$ diagrams with three external legs of type s . A large portion of them is obtained by dressing the constituents of the leading order triangle diagram with $1/N$ corrections. Before studying this class of diagrams, recall that the dressed ϕ - and s -propagators have a non-trivial $1/N$ correction due to the amplitudes A_ϕ , A_s , as well as due to the anomalous dimensions γ_ϕ , γ_s . We will account for the contribution related to $A_{\phi,s}$ later in this subsection, while for now we focus on studying the effect associated with the dressed vertex (100) and the anomalous dimensions $\gamma_{\phi,s}$ inherent to the dressed propagators.

Quite surprisingly, it turns out that various diagrams obtained by dressing the leading $\langle sss \rangle$ triangle can be grouped in such a way that the integrals over their internal vertices can be carried out using the uniqueness relation. We illustrate how it works now.

Dressing each of the three $\phi\phi s$ vertices of the leading $\langle sss \rangle$ triangle diagram gives



Here the vertex blob is determined by (100). In addition, each of the three internal ϕ -propagators and each of the three external s -propagators in the leading triangle diagram need to be endowed with the anomalous dimensions. The corresponding diagram is given by

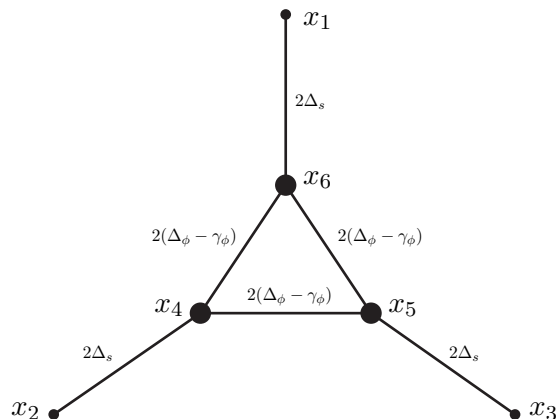


where we used the black blob propagator notation introduced in subsection V A.

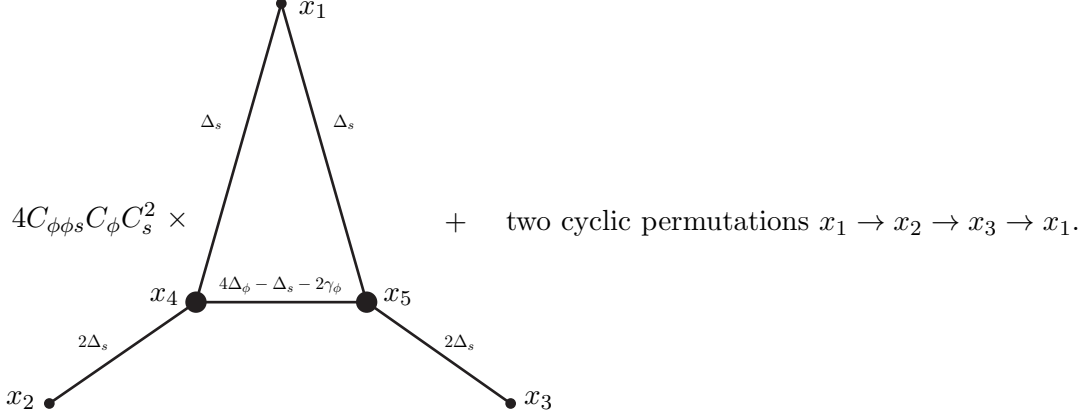
To avoid over-counting the contribution of the leading order triangle diagram, it should be subtracted from the above graphs. The remainder contributes to $W_{s3} \sim \mathcal{O}(1/N)$ which is the ultimate goal of our calculation. However, to avoid clutter we do not carry out these subtractions explicitly. They are done by default in what follows.

Remarkably, when summing the Feynman diagrams with identical skeleton structure, the anomalous dimensions of the propagators behave additively at $1/N$ order. This tremendous simplification holds because $\gamma_{\phi,s} \sim 1/N$, and therefore one can linearize a Feynman graph with respect to the anomalous dimensions.

For instance, each of the three dressed vertices of the leading order triangle diagram contributes a $1/N$ term associated with the second diagram on the r.h.s. of (100). Combining these terms with the above Feynman graph gives

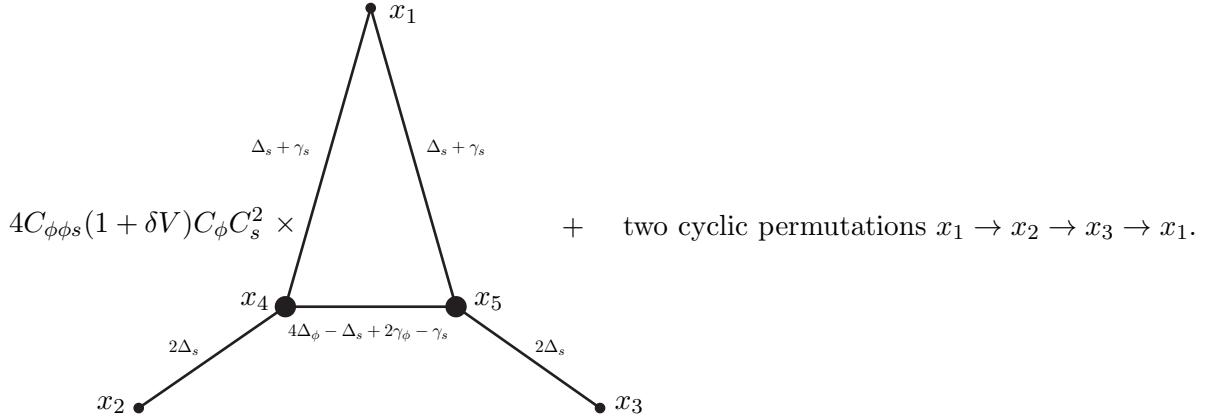


Since this relation between the diagrams is reliable up to $\mathcal{O}(1/N)$ order, we linearize over the γ_ϕ in the internal ϕ -propagators and retain the next-to-leading corrections only. They are given by the sum of three diagrams which are identical up to a permutation of the external legs

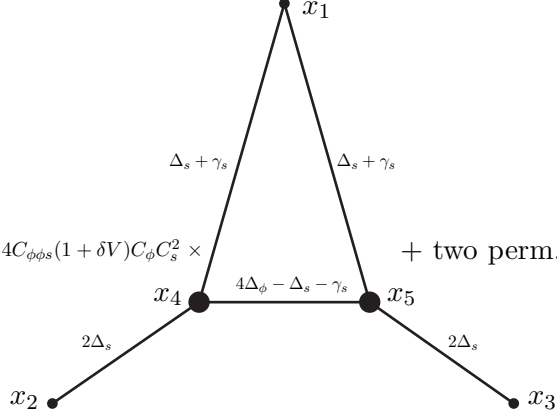


where we integrated over the unique vertex with the lines Δ_{ϕ} , Δ_{ϕ} , Δ_s and used (82). The factor of $\left(-\frac{2}{\sqrt{N}}\right)^2 NC_{\phi}C_s^2$ is associated with the Feynman rules for the vertices $x_{4,5}$, the closed ϕ -loop, and the leading order amplitudes of the ϕ - and s - propagators.

Furthermore, there is a contribution related to the conformal triangle on the r.h.s. of (100). There are three such terms, since there are three vertices in the leading order correlation function $\langle sss \rangle$,



As before only $\mathcal{O}(1/N)$ terms are eventually retained, and therefore the last two diagrams can be combined by simply adding the anomalous dimensions of the corresponding propagators



$$4C_{\phi\phi s}(1+\delta V)C_\phi C_s^2 \times \text{ + two perm.} = \frac{4C_{\phi\phi s}C_\phi C_s^2 U\left(\Delta_s, \frac{\Delta_s+\gamma_s}{2}, d-\frac{3\Delta_s+\gamma_s}{2}\right) U\left(\Delta_\phi+\frac{\gamma_s}{2}, \Delta_\phi-\frac{\gamma_s}{2}, \Delta_s\right)}{(|x_{13}||x_{12}|)^{\Delta_s+\gamma_s} |x_{23}|^{\Delta_s-\gamma_s}} \times (1+\delta V) \text{ + two permutations}$$

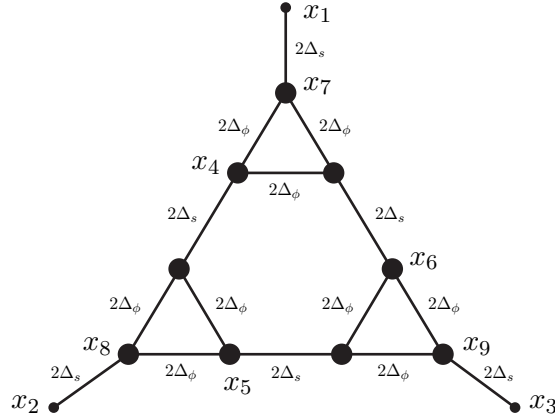
where the integrals over $x_{4,5}$ were carried out using the uniqueness relation. Note that only terms up to $\mathcal{O}(1/N)$ order are reliable, because we added the anomalous dimensions to combine the diagrams. Using (105), (106), the contribution to W_{s3} takes the form

$$\begin{aligned} 3\delta V + \hat{f} &= 3 \left(\delta V + \frac{U\left(\Delta_s, \frac{\Delta_s+\gamma_s}{2}, d-\frac{3\Delta_s+\gamma_s}{2}\right) U\left(\Delta_\phi+\frac{\gamma_s}{2}, \Delta_\phi-\frac{\gamma_s}{2}, \Delta_s\right)}{U\left(\Delta_s, \frac{\Delta_s}{2}, d-\frac{3\Delta_s}{2}\right) U\left(\Delta_\phi, \Delta_\phi, \Delta_s\right)} - 1 \right) \\ &= 3\delta V + \frac{6 \sin\left(\frac{\pi d}{2}\right) \Gamma(d) \left(-\frac{2}{d-4} + \pi \cot\left(\frac{\pi d}{2}\right) + H_{d-4}\right)}{N\pi \Gamma\left(\frac{d}{2}-1\right) \Gamma\left(\frac{d}{2}+1\right)} + \mathcal{O}(1/N^2), \end{aligned} \quad (107)$$

where H_n is the n th harmonic number. Expanding around $d=6$, yields

$$\hat{f} = -\frac{120}{N} + \mathcal{O}(d-6). \quad (108)$$

Another contribution to W_{s3} arises from the following diagram



Integrating over x_{4-9} through the use of uniqueness relation (50), and normalizing the external s legs according to (83), we obtain an additional contribution to W_{s3} of the form w_3/\tilde{C}_{s3} with

$$\begin{aligned} w_3 &= \frac{1}{C_s^{3/2}} \left(-\frac{2}{\sqrt{N}}\right)^9 N^3 C_\phi^9 C_s^6 U(\Delta_\phi, \Delta_\phi, \Delta_s)^3 U\left(\frac{\Delta_s}{2}, \Delta_s, d-\frac{3\Delta_s}{2}\right)^3 \hat{w}_3 \\ &= -\frac{64(d-3)^3}{N^{3/2}} C_\phi^3 C_s^{\frac{3}{2}} \hat{w}_3, \end{aligned} \quad (109)$$

where in the last line we used (105), and \hat{w}_3 is defined by the diagram¹⁵

$$= \frac{\hat{w}_3}{|x_{12}|^2 |x_{13}|^2 |x_{23}|^2}$$

Integrating both sides of this diagrammatic equation w.r.t. x_1 we obtain

$$\hat{w}_3 = \frac{U\left(3 - \frac{d}{2}, \frac{d}{2} - 1, d - 2\right)}{U(1, 1, d - 2)} v_3, \quad (110)$$

where v_3 is determined by the diagram

$$= \frac{v_3}{|x_{23}|^{6-d}}$$

Attaching propagator lines with powers $2d - 4$ to $x_{2,3}$, and integrating both sides of the obtained equation w.r.t. $x_{2,3}$, yields

$$v_3 = \frac{U\left(3 - \frac{d}{2}, \frac{d}{2} - 1, d - 2\right)}{U(1, 1, d - 2)} \tilde{v}_3(0), \quad (111)$$

where $\tilde{v}_3(\delta)$ is defined by the diagram

$$= \frac{\tilde{v}_3(\delta)}{|x_{23}|^{d-2+\delta}}$$

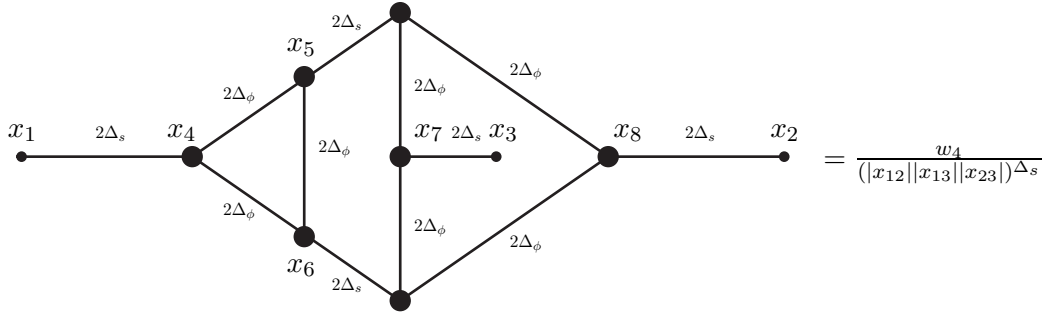
¹⁵ From now on we explicitly use the values (43) for the scaling dimensions $\Delta_{\phi,s}$. To get \hat{w}_3 from this diagram one needs to integrate over the three internal points. We already accounted for the amplitudes $C_{\phi,s}$ of the propagators and factors of $-2/\sqrt{N}$ coming from the interaction vertices.

Here we have introduced an auxiliary regulator, δ , in order to apply the integration by parts relation (the diagram itself is finite in $\delta \rightarrow 0$ limit). We relegate the details to Appendix B. Combining (85), (106), (113), (110), (111) gives the result

$$\frac{w_3}{\tilde{C}_{s^3}} = \frac{16(d-3)^2}{N} C_\phi^2 C_s \frac{U\left(3 - \frac{d}{2}, \frac{d}{2} - 1, d-2\right)^2}{U(1, 1, d-2)^2 U\left(\frac{d-2}{2}, \frac{d-2}{2}, 2\right)} \tilde{v}_3(0), \quad (112)$$

where $\tilde{v}_3(0)$ is given by (B9).

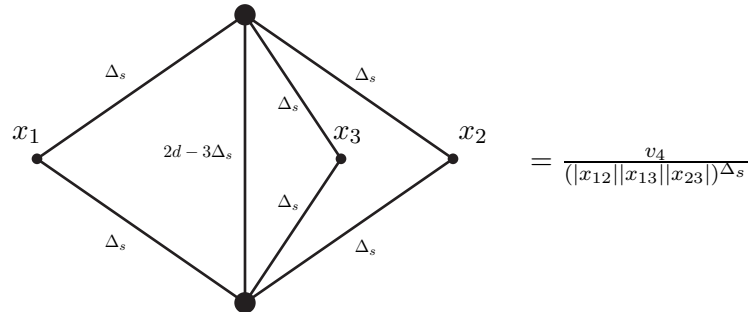
Next, we evaluate the following contribution to W_{s^3} represented by the 3-loop ‘bellows’¹⁶ diagram¹⁷



Normalizing the external s legs in accord with (83), and using the uniqueness relation (50) to integrate over the five points x_{4-8} , yields¹⁸

$$W_{s^3} \supset \frac{w_4}{\tilde{C}_{s^3}} = \frac{3}{2} \left(-\frac{2}{\sqrt{N}} \right)^4 N C_\phi^4 C_s^2 U(\Delta_\phi, \Delta_\phi, \Delta_s)^2 v_4, \quad (113)$$

where v_4 is defined by the following diagrammatic equation (the multiplicative factors of $-2/\sqrt{N}$ and $C_{\phi,s}$ in the vertices and propagators of this diagram should be stripped off, because we already took them into account)

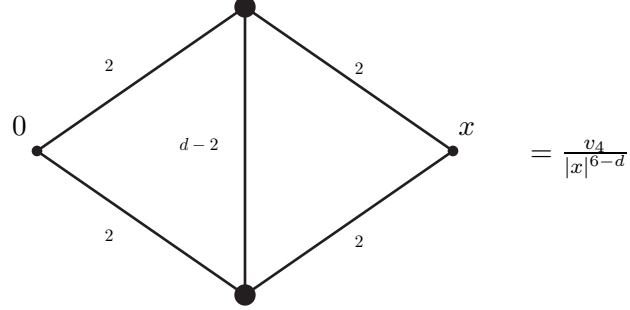


¹⁶ The name is based on the visual resemblance of the three-dimensional shape of this diagram to a bellows, see, *e.g.*, <https://en.wikipedia.org/wiki/Bellows>

¹⁷ We are grateful to anonymous referee at PRD who pointed out this diagram to us.

¹⁸ The symmetry factor of this diagram is 1/2, whereas its multiplicity is 3 due to the possibility of having the ϕ -triangle attached to each of the points x_{1-3} . Recall also that the contribution to W_{s^3} is obtained by dividing the value of w_4 by \tilde{C}_{s^3} , see (101).

Integrating both sides of this equation w.r.t. x_3 , we obtain (here we explicitly use the values (43) for the scaling dimensions $\Delta_{\phi,s}$)



This is the so-called self-energy diagram. It can be reduced to the known $\text{ChT}(\alpha, \beta)$ graph, given by eq. (16) in [26].¹⁹ To this end we perform an inversion transformation on the external point x and on both of the integrated vertices. This gives $v_4 = \text{ChT}(1, 1)$. Combining all together, we arrive at

$$\frac{w_4}{\tilde{C}_{s^3}} = \gamma_\phi \frac{3d(d-2) (\pi^2 - 6\psi^{(1)}(\frac{d}{2} - 1))}{4(d-4)}, \quad (114)$$

where $\psi^{(1)}$ is the first derivative of the digamma function. In particular,

$$\frac{w_4}{\tilde{C}_{s^3}} = -\frac{9}{2} \frac{1}{N} (d-4)^2 \psi^{(2)}(1) + \mathcal{O}((d-4)^3), \quad d \rightarrow 4, \quad (115)$$

$$\frac{w_4}{\tilde{C}_{s^3}} = -54 \frac{1}{N} (d-6) + \mathcal{O}((d-6)^2), \quad d \rightarrow 6. \quad (116)$$

The plot of (114) for the range of values $2 < d < 6$ is shown in figure 1.

To account for the contribution of the $\mathcal{O}(1/N)$ corrections, $A_{\phi,s}$, to the amplitudes of the dressed ϕ - and s -propagators, we simply add to W_{s^3} a term $3A_s + 3A_\phi$. Furthermore, there is an additional term $-\frac{3}{2}A_s$, associated with normalization (83) of the three external s legs. As a result, W_{s^3} takes the form

$$W_{s^3} = 3\delta V + \hat{f} + \frac{3}{2}A_s + 3A_\phi + \frac{w_3 + w_4}{\tilde{C}_{s^3}}. \quad (117)$$

Substituting (95), yields

$$W_{s^3} = 3W_{\phi\phi s} + \hat{f} + \frac{w_3 + w_4}{\tilde{C}_{s^3}}. \quad (118)$$

¹⁹ See Appendix B for details regarding the self-energy diagram, *e.g.*, (B7) for an explicit form of $\text{ChT}(\alpha, \beta)$.

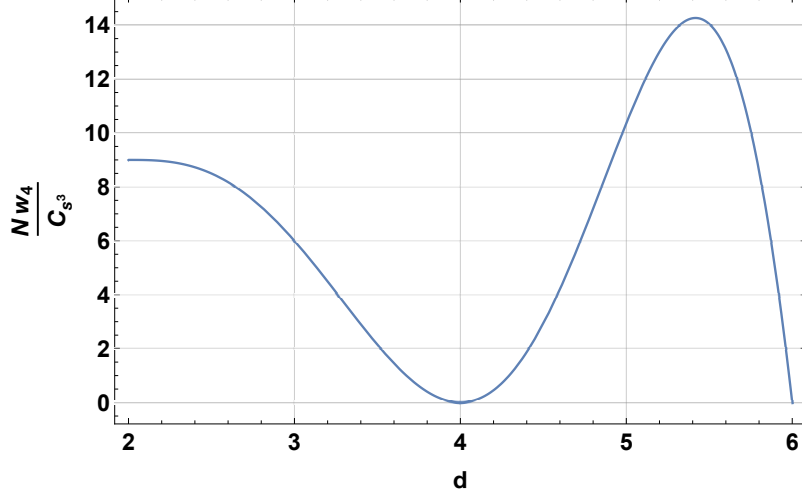


FIG. 1: Nw_4/\tilde{C}_{s^3} as a function of space-time dimension $2 < d < 6$.

Here w_3/\tilde{C}_{s^3} is given by (112), which we re-write as

$$\frac{w_3}{\tilde{C}_{s^3}} = b_3 \tilde{v}_3(0), \quad (119)$$

where $\tilde{v}_3(0)$ is calculated in Appendix B, and

$$b_3 = \frac{16(d-3)^2}{N} C_\phi^2 C_s \frac{U(3 - \frac{d}{2}, \frac{d}{2} - 1, d-2)^2}{U(1, 1, d-2)^2 U(\frac{d-2}{2}, \frac{d-2}{2}, 2)}. \quad (120)$$

In particular, it simplifies in the vicinity of $d = 4, 6$

$$b_3 = \frac{1}{N} \frac{(d-4)^3}{\pi^6} + \mathcal{O}((d-4)^4), \quad d \rightarrow 4, \quad (121)$$

$$b_3 = -\frac{1}{N} \frac{216(d-6)^3}{\pi^9} + \mathcal{O}((d-6)^4), \quad d \rightarrow 6. \quad (122)$$

Moreover, from (B9) we obtain

$$\tilde{v}_3(0) = 20\pi^6 \zeta(5) + \mathcal{O}(d-4), \quad d \rightarrow 4, \quad (123)$$

$$\tilde{v}_3(0) = -\frac{\pi^9}{(d-6)^3} + \mathcal{O}((d-6)^{-2}), \quad d \rightarrow 6. \quad (124)$$

The full expression for w_3/\tilde{C}_{s^3} is displayed in (130) below, where $\psi^{(n)}(x)$ is n th derivative of the digamma function $\psi^{(0)}(x) = \Gamma'(x)/\Gamma(x)$, and γ is the Euler constant. The plot of (130) for the range $2 \leq d \leq 6$ is shown in figure 2. There is an apparent singularity in $d = 3$, which is an artifact of our normalization. Note that \tilde{C}_{s^3} has a simple zero in $d = 3$.

The theory becomes free at the fixed point in the limit $d \rightarrow 4$, therefore $W_{s^3}(d \rightarrow 4)$ must

vanish.²⁰ Indeed, based on our (95), $W_{\phi\phi s}(d \rightarrow 4) = 0$, in agreement with [9, 10]. From (118) it then remains to show that $\frac{w_3+w_4}{\tilde{C}_{s^3}}(d \rightarrow 4) = 0$, which is indeed the case (in fact $w_{3,4}/\tilde{C}_{s^3}$ contributions vanish individually), as can be seen from (115), (119), (121), (123). Using (107) one can also verify that $\hat{f}(d=4) = 0$.

Moreover, it follows from (119), (122), (124) that in the vicinity of $d = 6$, we have

$$\frac{w_3}{\tilde{C}_{s^3}} = \frac{216}{N} + \mathcal{O}(d-6). \quad (125)$$

From (99), (108), (116), (118) and (125) we then obtain in $d = 6 - \epsilon$,

$$W_{s^3} = \frac{162}{N} + \mathcal{O}(\epsilon). \quad (126)$$

The same value for W_{s^3} was obtained in [7, 8] for the critical cubic model. This match between the OPE coefficients provides an additional non-trivial evidence for the equivalence between the models. In fact, it suggests existence of a wide class of universal relations between the $O(N)$ CFTs in general d , at least in the $1/N$ expansion. Some of these relations have been established in [9, 10] using the bootstrap method and without considering a particular Lagrangian or space-time dimension. Our findings suggest that the bootstrap approach to the $O(N)$ CFTs, initiated in [9, 10], might not be exhausted.²¹ Presumably it can be extended to unravel a larger class of universal relations, which hold regardless of the specific structure of the $O(N)$ invariant Hamiltonian at the fixed point. In fact, these relations could be valid in general d , and apply to all $O(N)$ symmetric CFTs with the same number of degrees of freedom, rather than just to the critical ϕ^4 vector model or cubic model of [7, 8]. A non-trivial match (126) of the OPE data to $1/N$ order in the case of apparently distinct models provides a partial evidence to this statement.

We plot the full result (118) for W_{s^3} in figure 3. It should be noticed that the lack of the refined result for the $\langle sss \rangle$ correlator has been particularly emphatic since the work of [9, 10], where the next-to-leading order value for the $\langle \phi\phi s \rangle$ three-point function was established. The new result (118) for the $\langle sss \rangle$ allowed us to subject the hypothesis of [7, 8] to a non-trivial test.

Finally, we would like to stress that while the results for the multi-loop diagrams, *e.g.*, the 4-loop triangle diagram (130), played a crucial role in the direct diagrammatic calculation of the $\langle sss \rangle$ three-point function at the next-to-leading order in the $1/N$ expansion, they have independent value, because diagrams of this type are ubiquitous in perturbative CFTs. Two additional useful

²⁰ We would like to thank Simone Giombi, Igor Klebanov and Gregory Tarnopolsky for discussing with us the $d = 4$ case. Their insight helped us to improve our previous version of the related calculation.

²¹ Recent advancements in bootstrap calculations in the $O(N)$ vector models have been reported in [42].

relations obtained in this section are the 3-loop trapezoid diagram v_3 , or equivalently \tilde{v}_3 (see also Appendix B) and the 3-loop bellow diagram (114). To best of our knowledge the analytic expressions for these diagrams do not appear in the literature.

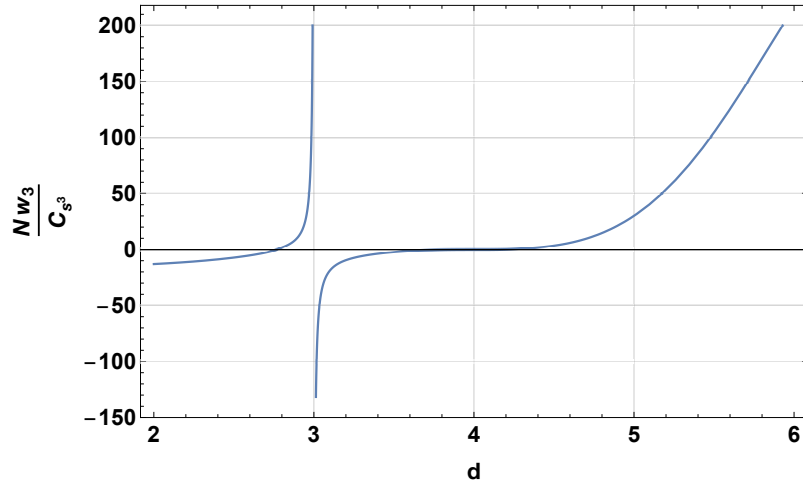


FIG. 2: Nw_3/\tilde{C}_{s^3} as a function of space-time dimension $2 < d < 6$. Our choice of normalization results in a pole, because \tilde{C}_{s^3} vanishes in $d = 3$.

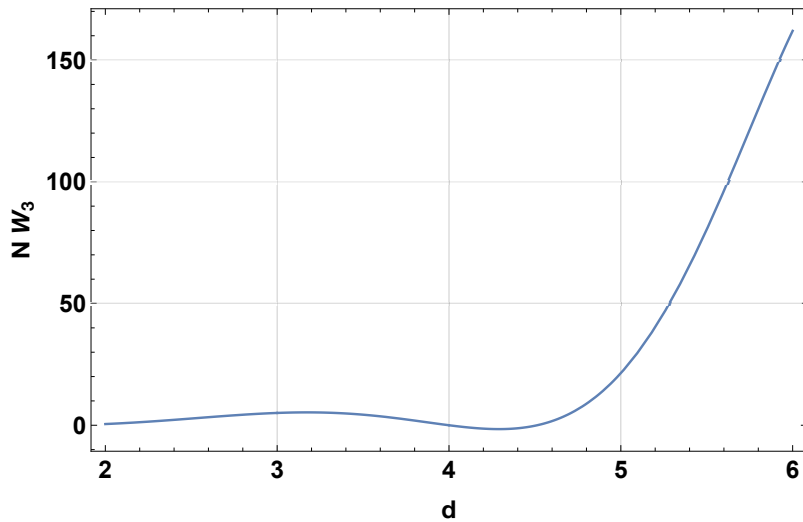


FIG. 3: The total $1/N$ correction W_{s^3} to $\langle sss \rangle$ as a function of space-time dimension $2 < d < 6$. Some of the values are $NW_{s^3}(d = 2) = 1/2$, $NW_{s^3}(d = 4) = 0$, $NW_{s^3}(d = 6) = 162$.

For convenience, we recapitulate the full answer for W_{s^3} , determined by (54), (74), (95), (97),

(107), (114), (118) and (119)

$$W_{s^3} = 3W_{\phi\phi s} + \hat{f} + \frac{w_3 + w_4}{\tilde{C}_{s^3}}, \quad (127)$$

$$W_{\phi\phi s} = \gamma_\phi \left(\frac{d(d-3)+4}{4-d} \left(H_{d-3} + \pi \cot\left(\frac{\pi d}{2}\right) \right) + \frac{16}{(d-4)^2} + \frac{6}{d-4} + \frac{2}{d-2} - 2d + 3 \right), \quad (128)$$

$$\hat{f} = \gamma_\phi \frac{6(d-1)(d-2)}{d-4} \left(H_{d-4} - \frac{2}{d-4} + \pi \cot\left(\frac{\pi d}{2}\right) \right), \quad (129)$$

$$\frac{w_3}{\tilde{C}_{s^3}} = \gamma_\phi \frac{2d(d-2)(d-3)}{(d-4)^2} \left(6\psi^{(1)}\left(\frac{d}{2}-1\right) - \psi^{(1)}(d-3) - \frac{\pi^2}{6} - H_{d-4} \left(H_{d-4} + 2\pi \cot\left(\frac{\pi d}{2}\right) \right) \right), \quad (130)$$

$$\frac{w_4}{\tilde{C}_{s^3}} = \gamma_\phi \frac{3d(d-2)(\pi^2 - 6\psi^{(1)}\left(\frac{d}{2}-1\right))}{4(d-4)}, \quad (131)$$

where $\psi^{(n)}$ is the n th derivative of the digamma function $\psi^{(0)}(x) = \Gamma'(x)/\Gamma(x)$, H_n is the n th harmonic number, and $\gamma_\phi \sim 1/N$ is given by (53).

We conclude this section by discussing a potential application of our results for the three-point function $\langle sss \rangle$ in the context of $3d/4d$ critical vector model/higher spin theory correspondence [43]. We find that in $d = 3$ the OPE coefficient vanishes up to the next-to-leading order in $1/N$,²²

$$W_{s^3}(d = 3) = 0 + \mathcal{O}(1/N^2). \quad (133)$$

It happens because of a rather non-trivial cancellation between the simple poles of two apparently unrelated terms in the expression for W_{s^3}

$$N\hat{f} = \frac{16}{\pi^2} \frac{1}{d-3} + \mathcal{O}((d-3)^0), \quad (134)$$

$$N\frac{w_3}{\tilde{C}_{s^3}} = -\frac{16}{\pi^2} \frac{1}{d-3} + \mathcal{O}((d-3)^0). \quad (135)$$

A large body of the literature, starting from the work of [43] was dedicated to studying the holographic correspondence between the critical $O(N)$ vector model in $d = 3$ and the type-A Vasiliev higher-spin theory in AdS_4 . While in this paper we do not do justice to properly reviewing related literature, we would like to point out that it is tempting to discuss our result (133) in the context of holographic correspondence. Indeed, the earlier works by [46, 47] (see also [48] for an extensive discussion of the holographic three-point functions) argue that to leading order in the large N expansion, the higher-spin theory in AdS_4 bulk implies that in $d = 3$

$$\langle sss \rangle = 0 + \mathcal{O}(1/N^{3/2}). \quad (136)$$

²² Most accurate available numerical values of the total $\langle sss \rangle$ OPE coefficient λ_{sss} in $d = 3$ were presented in [44, 45]

$$\lambda_{sss} \Big|_{O(2)} = 0.830914(32), \quad \lambda_{sss} \Big|_{O(3)} = 0.499(12). \quad (132)$$

This equation is in full agreement with the field theory dual, which in fact has been known since [9, 10], as we reviewed above in this section.

The new result (133) for the next-to-leading order $\langle sss \rangle$ raises a natural question whether the holographic work of [46, 47] extends to order $\mathcal{O}(1/N^{3/2})$. Notice that [46] shows that (136) is valid for the AdS_4 dual of *any* $O(N)$ CFT in $d = 3$. In particular, no assumption was made that the AdS_4 bulk is populated by the higher-spin fields of Vasiliev's theory [46]. In fact, it may happen that (133) holds for a large class of $O(N)$ CFTs in $d = 3$. Holography is a possible tool to check this conjecture. In particular, one can try to extend the holographic argument of [46] to the next-to-leading order in the $1/N$ expansion. A possible outcome $\langle sss \rangle = 0 + \mathcal{O}(1/N^{5/2})$ of a generic bulk calculation would be a strong evidence in favor of the holographic duality [43], and universality of the $W_{s,3}$ for a broad class of $O(N)$ CFTs in general dimension.

VI. DISCUSSION

In this work we explore the $O(N)$ critical vector model with quartic interaction in $2 \leq d \leq 6$ dimensions. In higher dimensions this model provides a nice illustration of the asymptotically safe quantum field theory, whereas in lower dimensions it is closely related to realistic systems such as the critical Ising model in 3D. While it is difficult to prove the existence of the fixed point in full generality, perturbative approach, ϵ - and large- N expansions confirm they exist in this model. Our calculations encompass the next-to-leading order analysis in the $1/N$ expansion and extend previously known results in a few ways.

We derive and perform consistency checks that provide an additional evidence for the existence of a non-trivial fixed point. Moreover, we continue non-perturbative studies of the emergent conformal field theory and use conformal techniques to calculate a new CFT data associated with the three-point functions of the fundamental scalar and Hubbard-Stratonovich fields. This helps to expand our understanding of a CFT describing critical ϕ^4 model in general dimension. Along the way we evaluate a number of conformal multi-loop diagrams up to and including 4 loops in general d . These diagrams are generic and have value in themselves since they are not restricted to the critical ϕ^4 model, but rather inherent to various CFTs.

In [7, 8] an alternative description of the critical $O(N)$ model in terms of $N + 1$ massless scalars with cubic interactions was proposed. It was explicitly shown that the scaling dimensions of various operators within the alternative description match the known results for the critical $O(N)$ theory. While our findings confirm the observations made in [7, 8], we find an additional

agreement between the next-to-leading coefficients of the $\langle sss \rangle$ three-point functions, previously unobserved in the literature.

In fact, it can be shown that all higher order correlation functions $\langle s(x_1) \cdots s(x_n) \rangle$, $n = 4, 5, \dots$ in both models match to leading order in the $1/N$ and ϵ expansion. In general, these correlators are entirely fixed by the 1PI vertices of the effective action. To leading order in the $1/N$ expansion these vertices are given by a single ϕ -loop with s -legs attached to it. In the ϕ^4 theory they have the following form

$$\Gamma_{\phi^4}^{\text{1PI}}(x_1, \dots, x_n) = N C_\phi^n C_s^{n/2} \left(-\frac{2}{\sqrt{N}} \right)^n \int \prod_{i=1}^n d^d x_i \mathcal{I}(x_1, \dots, x_n) s(x_1) \cdots s(x_n), \quad (137)$$

where $\mathcal{I}(x_1, \dots, x_n)$ is a space dependent structure representing the internal ϕ -loop, and the external s -legs are normalized according to (83). In the cubic model the same vertex equals to

$$\Gamma_{\text{cubic}}^{\text{1PI}}(x_1, \dots, x_n) = N C_\phi^{3n/2} (-g_1)^n \int \prod_{i=1}^n d^d x_i \mathcal{I}(x_1, \dots, x_n) s(x_1) \cdots s(x_n), \quad (138)$$

where the fixed point value of the $\phi\phi s$ coupling constant is given by [7]

$$g_1 = \sqrt{\frac{6\epsilon(4\pi)^3}{N}} \left(1 + \mathcal{O}\left(\frac{1}{N}, \epsilon\right) \right). \quad (139)$$

In (138) we took into account that the s field in the cubic model is canonically normalized, and therefore the amplitude of its propagator in position space equals C_ϕ . Note that (137) and (138) share the same structure $\mathcal{I}(x_1, \dots, x_n)$ because the 1PI diagrams are identical up to an overall constant prefactor, which is explicitly written down in both cases. It then remains to show that these constants are identical. Indeed,

$$\left(\sqrt{N} \frac{g_1}{2} \right)^2 \frac{C_\phi}{C_s} = 1 + \mathcal{O}\left(\frac{1}{N}, \epsilon\right). \quad (140)$$

The above matches support the equivalence suggested in [7, 8] between the critical ϕ^4 vector model and the critical cubic model in $d = 6 - \epsilon$ dimensions. Based on these findings we propose that the new result for $W_{s,3}$, which did not appear in the literature before our work, is in fact universally applicable to a large class of $O(N)$ CFTs. Therefore we interpret the match between the $W_{s,3}$ coefficients of the critical ϕ^4 model and the critical cubic model in $d = 6 - \epsilon$ dimensions as a particular manifestation of this universality. Moreover, we suspect that it might be possible to systematically derive additional universal relations, at least in the $1/N$ expansion, thereby replacing the equivalence of [7, 8] by a universally valid bootstrap statement.²³

²³ Another reason to believe in the universality of the critical $O(N)$ vector models in general d is due to the observation

Furthermore, we notice that the critical $O(N)$ model in higher dimensions does have certain unphysical features. The well-known ϵ -expansion shows that the coupling constant at the Wilson-Fisher fixed point is negative in $4 + \epsilon$ dimensions [1]. This means that the potential is unbounded from below for large values of the field. However, perturbative calculations in $1/N$ do not reveal any sign of instability at the level of the correlation functions. Thus, for instance, unitarity bounds are satisfied. Of course, this argument only shows that the vacuum state of the theory is metastable if the instability observed within ϵ -expansion persists in the $\epsilon \rightarrow 1$ limit.

Indeed, in the recent work [11] the authors provide a non-perturbative argument in favour of instability of the model. Their analysis rests on the observation that the path integral in the large- N limit is entirely dominated by the saddle point. The corresponding saddle point equation is Weyl invariant at the fixed point, and therefore admits a family of solutions parametrized by size and location. This type of large- N instantons was previously observed in the critical ϕ^6 model in three dimensions [50]. In particular, it was argued that the instantons and associated instability of the critical ϕ^6 model can be used as a toy model towards holographic resolution of the singularity and conformal factor problems in quantum cosmology. It would be interesting to explore these aspects in the context of critical ϕ^4 model.

Remarkably, the critical $O(N)$ vector models exhibit peculiar behaviour when coupled to a thermal bath [51]. We hope that certain results presented in this paper might be of help towards understanding this behaviour in lower dimensions. Progress in this direction will be reported elsewhere [52].

Acknowledgements

We thank Noam Chai, Soumangsu Chakraborty, Johan Henriksson, Zohar Komargodski and Anastasios Petkou for helpful discussions and correspondence. We would like to express our special thanks of gratitude to Simone Giombi, Igor Klebanov and Gregory Tarnopolsky for numerous comments and stimulating correspondence which helped us to improve our results and their presentation. This work is partially supported by the Binational Science Foundation (grant No. 2016186), the Israeli Science Foundation Center of Excellence (grant No. 2289/18) and by the

related to the behavior of $W_{s,3}$ coefficient when extrapolated to $d = 8$. While the vector model in $d = 8$ is manifestly non-unitary, since the scaling dimension of the operator s is below the unitarity bound, we can nevertheless formally compare our result $NW_{s,3}(d = 8) = -950$ with a similar calculation in the exotic critical model in $8 - \epsilon$ dimensions [49]. We find a precise match with $NW_{s,3}$ calculated in [49]. We are grateful to Simone Giombi, Igor Klebanov and Gregory Tarnopolsky for letting us know about [49] and suggesting to compare the results.

Quantum Universe I-CORE program of the Israel Planning and Budgeting Committee (grant No. 1937/12).

Appendix A: Callan-Symanzik equations

In this appendix we use the Callan-Symanzik equation to derive various relations between the counterterms δ_ϕ , $\hat{\delta}_s$, $\hat{\delta}_4$, and the anomalous dimensions γ_ϕ , γ_s . In particular we establish the identity (16) satisfied by the counterterms δ_s and $\hat{\delta}_s$. The calculation is carried out for the model (12) with mass set to zero $m = 0$. Depending on the dimension d the model is assumed to sit either at the UV or IR fixed point.

Let us start with the two-point function for the renormalized field ϕ ,

$$\langle \tilde{\phi}(p)\tilde{\phi}(q) \rangle = (2\pi)^d \delta(p+q) \left(\frac{1}{p^2} + \text{loop corrections} + \frac{-p^2 \delta_\phi}{(p^2)^2} \right). \quad (\text{A1})$$

It satisfies the Callan-Symanzik equation

$$\left(\mu \frac{\partial}{\partial \mu} + 2\gamma_\phi \right) \langle \tilde{\phi}(p)\tilde{\phi}(q) \rangle = 0, \quad (\text{A2})$$

which leads to

$$\gamma_\phi = \frac{1}{2} \mu \frac{\partial}{\partial \mu} \delta_\phi + \mathcal{O}(1/N^2). \quad (\text{A3})$$

Similarly, the Callan-Symanzik equation for the Hubbard-Stratonovich field reads

$$\left(\mu \frac{\partial}{\partial \mu} + 2\gamma_s \right) \langle \tilde{s}(p)\tilde{s}(q) \rangle = 0, \quad (\text{A4})$$

Here we have

$$\langle \tilde{s}(p)\tilde{s}(q) \rangle = (2\pi)^d \delta(p+q) \left(-\frac{1}{2B(p)} + \text{loop corrections} + \frac{\hat{\delta}_s}{2B(p)} \right), \quad (\text{A5})$$

where B is given by (46). At the order $\mathcal{O}(1/N)$ the loop corrections to the $\langle \tilde{s}\tilde{s} \rangle$ propagator in (A5) contain dependence on the renormalization scale μ , due to contributions from the $\phi\phi s$ interaction vertex counterterm, and the ϕ field strength renormalization counterterm. Denoting the associated terms with $\mathcal{L}_s(\mu)$ and using (A4) we obtain

$$\gamma_s = \frac{1}{2} \mu \frac{\partial}{\partial \mu} (\hat{\delta}_s + 2B\mathcal{L}_s) + \mathcal{O}(1/N^2). \quad (\text{A6})$$

Finally, for the three-point function

$$\begin{aligned} \langle \tilde{\phi}(p_1)\tilde{\phi}(p_2)\tilde{s}(q) \rangle &= (2\pi)^d \delta(p_1 + p_2 + q) \frac{1}{p_1^2} \frac{1}{p_2^2} \frac{-1}{2B(q)} \\ &\times \left(-\frac{2}{\sqrt{N}} + \text{loop corrections} - \frac{2}{\sqrt{N}} \frac{\hat{\delta}_4}{\sqrt{g_4}} + (-2\delta_\phi - \hat{\delta}_s) \left(-\frac{2}{\sqrt{N}} \right) \right), \end{aligned} \quad (\text{A7})$$

the Callan-Symanzik equation at the fixed point takes the form

$$\left(\mu \frac{\partial}{\partial \mu} + 2\gamma_\phi + \gamma_s \right) \langle \tilde{\phi}(p_1) \tilde{\phi}(p_2) \tilde{s}(q) \rangle = 0. \quad (\text{A8})$$

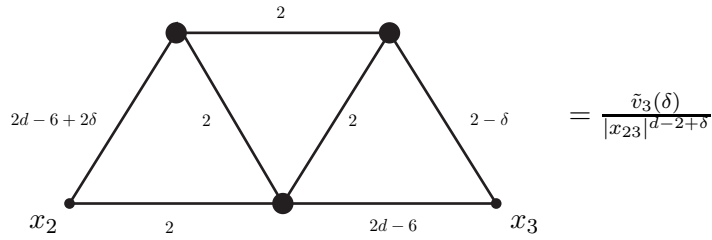
As a result, we obtain

$$\mu \frac{\partial}{\partial \mu} \left(\delta_s - \hat{\delta}_s + 2B\mathcal{L}_s \right) = 0 + \mathcal{O}(1/N^2), \quad (\text{A9})$$

where we substituted (A3), (A6) and used (13).

Appendix B: Calculation of the trapezoid diagram

In this appendix we calculate the trapezoid diagram $\tilde{v}_3(\delta)$ defined by (111). For completeness we reproduce here the defining diagram



It turns out that this diagram is quite ubiquitous, because various conformal graphs can be reduced to the trapezoid form through the use of conformal techniques, see for instance equations (4.345) and (4.346) in [30]. Although we did not find an explicit analytic expression for this diagram in the literature, the diagrammatic identity (4.345) in [30] suggests the following relation $\tilde{v}_3(0) = \frac{U(1,2,d-3)}{U(\frac{d}{2}-1,\frac{d}{2}-1,2)^2} \times \lim_{\lambda \rightarrow 0} (4.346)$. The direct calculation of $\tilde{v}_3(0)$ in this Appendix matches this result.

To calculate the trapezoid graph we use the following relation obtained by integration by parts [53], see also [36, 37]

$$\begin{aligned}
& (d - 2\alpha_1 - \alpha_2 - \alpha_3) \times \text{Diagram 1} = \alpha_2 \times \text{Diagram 2} - \alpha_2 \times \text{Diagram 3} \\
& + \alpha_3 \times \text{Diagram 4} - \alpha_3 \times \text{Diagram 5}
\end{aligned}$$

We apply this relation to the top left vertex of the \tilde{v}_3 diagram (with $\alpha_1 = 1$, $\alpha_2 = d - 3 + \delta$, $\alpha_3 = 1$), getting a sum of four terms. Then we use the propagator merging relation (48) to integrate over one of the vertices in the first three of those terms. As a result, the first three terms acquire the form of a self-energy diagram, and the fourth term acquires the form of a self-energy diagram with a line attached to the left-hand vertex. These self-energy diagrams can be brought to a similar form by an inversion transformation around the right-hand vertex. In the end we obtain

$$\begin{aligned}
\tilde{v}_3(\delta) = & -\frac{1}{\delta} \left[(U(d - 3 + \delta, 2, 1 - \delta) + (d - 3 + \delta)U(d - 2 + \delta, 1, 1 - \delta)) d_1 \right. \\
& \left. - U\left(2, 1 - \frac{\delta}{2}, d - 3 + \frac{\delta}{2}\right) d_2 - (d - 3 + \delta)U\left(d - 2 + \delta, 1 - \frac{\delta}{2}, 1 - \frac{\delta}{2}\right) d_3 \right], \tag{B1}
\end{aligned}$$

where we denoted

$$d_1 = F\left(\frac{d}{2} - 1 + \delta, \frac{d}{2} - 1 - \frac{\delta}{2}\right), \tag{B2}$$

$$d_2 = F\left(d - 3 + \delta, \frac{d}{2} - 1 - \frac{\delta}{2}\right), \tag{B3}$$

$$d_3 = F\left(1, d - 3 + \frac{\delta}{2}\right) \tag{B4}$$

for the function $F(\alpha, \beta)$ defined by the self-energy diagram

$$= \frac{F(\alpha, \beta)}{|x_{12}|^{2(3+\alpha+\beta-d)}}$$

To calculate this diagram we can again use the integration by parts relation for the top vertex, with $\alpha_1 = 1$, $\alpha_2 = \alpha$, $\alpha_3 = \beta$, after which all the remaining integrals can be straightforwardly taken using (48). As a result, we obtain

$$F(\alpha, \beta) = \frac{U(1, 1, d-2)}{d-2-\alpha-\beta} \left[\alpha \left(U(\alpha+1, \beta, d-\alpha-\beta-1) - U\left(\alpha+1, \beta+2-\frac{d}{2}, \frac{3d}{2}-\alpha-\beta-3\right) \right) + \beta \left(U(\alpha, \beta+1, d-\alpha-\beta-1) - U\left(\alpha+2-\frac{d}{2}, \beta+1, \frac{3d}{2}-\alpha-\beta-3\right) \right) \right]. \quad (\text{B5})$$

This diagram is dual by Fourier transform to the ChT diagram given by eq. (16) in [26], as can be checked explicitly

$$F(\alpha, \beta) = \frac{A(1)^3 A(\alpha) A(\beta)}{A(3+\alpha+\beta-d)} \text{ChT} \left(\frac{d}{2} - \alpha, \frac{d}{2} - \beta \right), \quad (\text{B6})$$

where

$$\text{ChT}(\alpha, \beta) = \frac{\pi^d A(d-2) \left(\frac{A(2-\alpha)A(\alpha)}{(1-\beta)(\alpha+\beta-2)} + \frac{A(\alpha+\beta-1)A(-\alpha-\beta+3)}{(\alpha-1)(\beta-1)} + \frac{A(2-\beta)A(\beta)}{(1-\alpha)(\alpha+\beta-2)} \right)}{\Gamma\left(\frac{d}{2}-1\right)}, \quad (\text{B7})$$

$$A(\Delta) = \frac{\Gamma\left(\frac{d}{2}-\Delta\right)}{\Gamma(\Delta)}. \quad (\text{B8})$$

As a result, from (B1) we obtain

$$\begin{aligned} \tilde{v}_3(0) &= \frac{-2^{4-d} \pi^{\frac{3d}{2}+\frac{5}{2}}}{(d-4) \sin^2\left(\frac{\pi d}{2}\right) \Gamma\left(\frac{d-3}{2}\right) \Gamma(d-2)} \\ &\times \left(\psi^{(1)}(d-3) - 6\psi^{(1)}\left(\frac{d}{2}-1\right) + H_{d-4} \left(H_{d-4} + 2\pi \cot\left(\frac{\pi d}{2}\right) \right) + \frac{\pi^2}{6} \right). \end{aligned} \quad (\text{B9})$$

The ϵ -expansion of the trapezoid diagram in $d = 4 - 2\epsilon$ dimensions was carried out in [36] (see eq. (19) therein) and [37] (see eq. (2.24) therein) to $\mathcal{O}(\epsilon^2)$ order.²⁴ Hence, we can test our result (B9) by substituting $d = 4 - 2\epsilon$, expanding in ϵ and comparing with [36, 37].²⁵ Performing the comparison we obtain a precise match to all available orders (*i.e.*, up to $\mathcal{O}(\epsilon^2)$) of the ϵ -expansion.

²⁴ Conventions of these references are slightly different from ours. One would need to set $a_1 = a_4 = -2$, $a_2 = a_3 = a_5 = a_6 = a_7 = 0$, and keep in mind that those references put the label equal to a half of the exponent on top of the propagator lines. In conventions of [36, 37] there is also a factor of $\pi^{-\frac{d}{2}}$ in each vertex.

²⁵ We thank Simone Giombi, Igor Klebanov and Gregory Tarnopolsky for the related discussion.

-
- [1] S. Weinberg, “Critical Phenomena for Field Theorists,” doi:10.1007/978-1-4684-0931-4-1
- [2] S. Weinberg, “Ultraviolet divergences in quantum theories of gravitation,” in “General relativity” S. Hawking, W. Israel (Ed.), Cambridge University Press (1979).
- [3] S. M. Christensen and M. J. Duff, “Quantum Gravity in Two + ϵ Dimensions,” Phys. Lett. **79B**, 213 (1978). doi:10.1016/0370-2693(78)90225-3
- [4] R. Gastmans, R. Kallosh and C. Truffin, “Quantum Gravity Near Two-Dimensions,” Nucl. Phys. B **133**, 417 (1978). doi:10.1016/0550-3213(78)90234-1
- [5] A. Eichhorn, “Status of the asymptotic safety paradigm for quantum gravity and matter,” Found. Phys. **48**, no. 10, 1407 (2018) doi:10.1007/s10701-018-0196-6 [arXiv:1709.03696 [gr-qc]].
- [6] K. G. Wilson and M. E. Fisher, “Critical exponents in 3.99 dimensions,” Phys. Rev. Lett. **28**, 240 (1972). doi:10.1103/PhysRevLett.28.240
- [7] L. Fei, S. Giombi and I. R. Klebanov, “Critical $O(N)$ models in $6 - \epsilon$ dimensions,” Phys. Rev. D **90**, no. 2, 025018 (2014) doi:10.1103/PhysRevD.90.025018 [arXiv:1404.1094 [hep-th]].
- [8] L. Fei, S. Giombi, I. R. Klebanov and G. Tarnopolsky, “Three loop analysis of the critical $O(N)$ models in $6-\epsilon$ dimensions,” Phys. Rev. D **91**, no. 4, 045011 (2015) doi:10.1103/PhysRevD.91.045011 [arXiv:1411.1099 [hep-th]].
- [9] A. C. Petkou, “ $C(T)$ and $C(J)$ up to next-to-leading order in $1/N$ in the conformally invariant $O(N)$ vector model for $2 < d < 4$,” Phys. Lett. B **359**, 101 (1995) doi:10.1016/0370-2693(95)00936-F [hep-th/9506116].
- [10] A. Petkou, “Conserved currents, consistency relations and operator product expansions in the conformally invariant $O(N)$ vector model,” Annals Phys. **249**, 180 (1996) doi:10.1006/aphy.1996.0068 [hep-th/9410093].
- [11] S. Giombi, R. Huang, I. R. Klebanov, S. S. Pufu and G. Tarnopolsky, “The $O(N)$ Model in $4 < d < 6$: Instantons and Complex CFTs” arXiv:1910.02462 [hep-th].
- [12] G. 't Hooft, “A Planar Diagram Theory for Strong Interactions,” Nucl. Phys. B **72**, 461 (1974). doi:10.1016/0550-3213(74)90154-0
- [13] E. Witten, “Baryons in the $1/n$ Expansion,” Nucl. Phys. B **160**, 57 (1979). doi:10.1016/0550-3213(79)90232-3
- [14] J. M. Maldacena, “The Large N limit of superconformal field theories and supergravity,” Int. J. Theor. Phys. **38**, 1113 (1999) [Adv. Theor. Math. Phys. **2**, 231 (1998)] doi:10.1023/A:1026654312961, 10.4310/ATMP.1998.v2.n2.a1 [hep-th/9711200].
- [15] E. Witten, “Anti-de Sitter space and holography,” Adv. Theor. Math. Phys. **2**, 253 (1998) doi:10.4310/ATMP.1998.v2.n2.a2 [hep-th/9802150].
- [16] S. S. Gubser, I. R. Klebanov and A. M. Polyakov, “Gauge theory correlators from noncritical string theory,” Phys. Lett. B **428**, 105 (1998) doi:10.1016/S0370-2693(98)00377-3 [hep-th/9802109].

- [17] S. Giombi, S. Minwalla, S. Prakash, S. P. Trivedi, S. R. Wadia and X. Yin, “Chern-Simons Theory with Vector Fermion Matter,” *Eur. Phys. J. C* **72**, 2112 (2012) doi:10.1140/epjc/s10052-012-2112-0 [arXiv:1110.4386 [hep-th]].
- [18] O. Aharony, S. Giombi, G. Gur-Ari, J. Maldacena and R. Yacoby, “The Thermal Free Energy in Large N Chern-Simons-Matter Theories,” *JHEP* **1303**, 121 (2013) doi:10.1007/JHEP03(2013)121 [arXiv:1211.4843 [hep-th]].
- [19] S. Yokoyama, “Chern-Simons-Fermion Vector Model with Chemical Potential,” *JHEP* **1301**, 052 (2013) doi:10.1007/JHEP01(2013)052 [arXiv:1210.4109 [hep-th]].
- [20] S. Jain, M. Mandlik, S. Minwalla, T. Takimi, S. R. Wadia and S. Yokoyama, “Unitarity, Crossing Symmetry and Duality of the S-matrix in large N Chern-Simons theories with fundamental matter,” *JHEP* **1504**, 129 (2015) doi:10.1007/JHEP04(2015)129 [arXiv:1404.6373 [hep-th]].
- [21] M. Geracie, M. Goykhman and D. T. Son, “Dense Chern-Simons Matter with Fermions at Large N,” *JHEP* **1604**, 103 (2016) doi:10.1007/JHEP04(2016)103 [arXiv:1511.04772 [hep-th]].
- [22] M. Goykhman, “Large N Thirring Matter in Three Dimensions,” *JHEP* **1607**, 034 (2016) doi:10.1007/JHEP07(2016)034 [arXiv:1605.08449 [hep-th]].
- [23] S. Giombi, G. Tarnopolsky and I. R. Klebanov, “On C_J and C_T in Conformal QED,” *JHEP* **1608**, 156 (2016) doi:10.1007/JHEP08(2016)156 [arXiv:1602.01076 [hep-th]].
- [24] G. Parisi, “The theory of non-renormalizable interactions: The large N expansion,” *Nucl. Phys. B* **100**, 368 (1975). doi.org:10.1016/0550-3213(75)90624-0
- [25] A. N. Vasiliev, Y. M. Pismak and Y. R. Khonkonen, “Simple Method of Calculating the Critical Indices in the $1/N$ Expansion,” *Theor. Math. Phys.* **46**, 104 (1981) [*Teor. Mat. Fiz.* **46**, 157 (1981)]. doi:10.1007/BF01030844
- [26] A. N. Vasiliev, Y. M. Pismak and Y. R. Khonkonen, “ $1/N$ Expansion: Calculation of the Exponents η and ν in the Order $1/N^2$ for Arbitrary Number of Dimensions,” *Theor. Math. Phys.* **47**, 465 (1981) [*Teor. Mat. Fiz.* **47**, 291 (1981)]. doi:10.1007/BF01019296
- [27] A. Vasiliev and M. Nalimov, “Analog of Dimensional Regularization for Calculation of the Renormalization Group Functions in the $1/n$ Expansion for Arbitrary Dimension of Space,” *Theor. Math. Phys.* **55**, 423-431 (1983) doi:10.1007/BF01015800
- [28] S. S. Gubser, C. Jepsen, S. Parikh and B. Trundy, “ $O(N)$ and $O(N)$ and $O(N)$,” *JHEP* **1711**, 107 (2017) doi:10.1007/JHEP11(2017)107 [arXiv:1703.04202 [hep-th]].
- [29] A. Vasiliev, Y. Pismak and Y. Khonkonen, “ $1/N$ expansion: calculation of the exponent η in the order $1/N^3$ by the conformal bootstrap method,” *Theor. Math. Phys.* **50**, 127-134 (1982) doi:10.1007/BF01015292
- [30] A. Vasilev, “The field theoretic renormalization group in critical behavior theory and stochastic dynamics”
- [31] J. Gracey, “Large N_f quantum field theory,” *Int. J. Mod. Phys. A* **33**, no.35, 1830032 (2019) doi:10.1142/S0217751X18300326 [arXiv:1812.05368 [hep-th]].

- [32] A. Kotikov and S. Teber, “Multi-loop techniques for massless Feynman diagram calculations,” *Phys. Part. Nucl.* **50**, no.1, 1-41 (2019) doi:10.1134/S1063779619010039 [arXiv:1805.05109 [hep-th]].
- [33] S. E. Derkachov and A. N. Manashov, “The Simple scheme for the calculation of the anomalous dimensions of composite operators in the $1/N$ expansion,” *Nucl. Phys. B* **522**, 301 (1998) doi:10.1016/S0550-3213(98)00103-5 [hep-th/9710015].
- [34] M. D’eramo, L. Peliti, G. Parisi, “On Calculations in conformal invariant field theories,” *Lett. Nuovo Cim.* **2** (1971) 878. doi:10.1007/BF02774121
- [35] K. Symanzik, “On Calculations in conformal invariant field theories,” *Lett. Nuovo Cim.* **3** (1972) 734. doi:10.1007/BF02824349
- [36] D. I. Kazakov, “Calculation Of Feynman Integrals By The Method Of ‘uniqueness’,” *Theor. Math. Phys.* **58**, 223 (1984) [*Teor. Mat. Fiz.* **58**, 343 (1984)]. doi:10.1007/BF01018044
- [37] D. I. Kazakov, “Analytical Methods For Multiloop Calculations: Two Lectures On The Method Of Uniqueness,” JINR-E2-84-410.
- [38] V. Belokurov and N. Usyukina, “An algorithm for calculating massless Feynman diagrams,” *Theor. Math. Phys.* **79**, 385-391 (1989) doi:10.1007/BF01015778
- [39] M. Ciuchini, S. E. Derkachov, J. Gracey and A. Manashov, “Computation of quark mass anomalous dimension at $O(1/N^2(f))$ in quantum chromodynamics,” *Nucl. Phys. B* **579**, 56-100 (2000) doi:10.1016/S0550-3213(00)00209-1 [arXiv:hep-ph/9912221 [hep-ph]].
- [40] K. Lang and W. Ruhl, “Critical nonlinear $O(N)$ sigma models at $2 < d < 4$: The Degeneracy of quasiprimary fields and its resolution,” *Z. Phys. C* **61**, 495 (1994). doi:10.1007/BF01413189
- [41] T. Leonhardt and W. Ruhl, “The Minimal conformal $O(N)$ vector sigma model at $d = 3$,” *J. Phys. A* **37**, 1403 (2004) doi:10.1088/0305-4470/37/4/023 [hep-th/0308111].
- [42] L. F. Alday, J. Henriksson and M. van Loon, “An alternative to diagrams for the critical $O(N)$ model: dimensions and structure constants to order $1/N^2$,” *JHEP* **01**, 063 (2020) doi:10.1007/JHEP01(2020)063 [arXiv:1907.02445 [hep-th]].
- [43] I. Klebanov and A. Polyakov, “AdS dual of the critical $O(N)$ vector model,” *Phys. Lett. B* **550**, 213-219 (2002) doi:10.1016/S0370-2693(02)02980-5 [arXiv:hep-th/0210114 [hep-th]].
- [44] F. Kos, D. Poland, D. Simmons-Duffin and A. Vichi, “Precision Islands in the Ising and $O(N)$ Models,” *JHEP* **08**, 036 (2016) doi:10.1007/JHEP08(2016)036 [arXiv:1603.04436 [hep-th]].
- [45] S. M. Chester, W. Landry, J. Liu, D. Poland, D. Simmons-Duffin, N. Su and A. Vichi, “Carving out OPE space and precise $O(2)$ model critical exponents,” [arXiv:1912.03324 [hep-th]].
- [46] A. C. Petkou, “Evaluating the AdS dual of the critical $O(N)$ vector model,” *JHEP* **03**, 049 (2003) doi:10.1088/1126-6708/2003/03/049 [arXiv:hep-th/0302063 [hep-th]].
- [47] E. Sezgin and P. Sundell, “Holography in 4D (super) higher spin theories and a test via cubic scalar couplings,” *JHEP* **07**, 044 (2005) doi:10.1088/1126-6708/2005/07/044 [arXiv:hep-th/0305040 [hep-th]].
- [48] S. Giombi and X. Yin, “Higher Spin Gauge Theory and Holography: The Three-Point Functions,” *JHEP* **09**, 115 (2010) doi:10.1007/JHEP09(2010)115 [arXiv:0912.3462 [hep-th]].

- [49] J. Gracey, “Six dimensional QCD at two loops,” *Phys. Rev. D* **93**, no.2, 025025 (2016) doi:10.1103/PhysRevD.93.025025 [arXiv:1512.04443 [hep-th]].
- [50] M. Smolkin and N. Turok, “Dual description of a 4d cosmology,” arXiv:1211.1322 [hep-th].
- [51] N. Chai, S. Chaudhuri, C. Choi, Z. Komargodski, E. Rabinovici and M. Smolkin, “Thermal Order in Conformal Theories,” [arXiv:2005.03676 [hep-th]].
- [52] In progress.
- [53] K. Chetyrkin and F. Tkachov, “Integration by Parts: The Algorithm to Calculate beta Functions in 4 Loops,” *Nucl. Phys. B* **192**, 159-204 (1981) doi:10.1016/0550-3213(81)90199-1